PAPER

Check for updates

A supramolecular magnetic and multifunctional Titriplex V-grafted chitosan organocatalyst for the synthesis of acridine-1,8-diones and 2-amino-3-cyano-4H-pyran derivatives†

Najmeh Hassanzadeh, Mohammad G. Dekamin ®* and Ehsan Valiey ®

In this research, a new supramolecular magnetic modified chitosan, namely, Fe_3O_4@CS−TDI−Titriplex V, was designed and prepared conveniently by grafting diethylenetriaminepentaacetic acid (Titriplex V) onto a biopolymeric chitosan backbone having urethane, urea, ester and amide functional groups. The obtained magnetic biopolymeric nanomaterial was properly characterized by different spectroscopic, microscopic or analytical methods including FTIR spectroscopy, EDX spectroscopy, XRD, FESEM, TG-DTA and VSM. The application of the supramolecular Fe_3O_4@CS−TDI−Titriplex V nanocomposite as a heterogeneous solid acidic organocatalyst was investigated to promote the three-component synthesis of both acridinediones and 2-amino-3-cyano-4H-pyran derivatives as important pharmaceutical scaffolds under green conditions. The obtained nanomaterial exhibited proper catalytic activity in the above mentioned transformations through multicomponent reaction (MCR) strategies. The reactions proceeded very well in the presence of the Fe_3O_4@CS−TDI−Titriplex V solid acid nanomaterial in EtOH to afford the corresponding acridinediones and 2-amino-3-cyano-4H-pyran derivatives in high to excellent yields. The key advantages of the present protocol include the use of a renewable, biopolymeric and biodegradable solid acid as well as a simple procedure for the preparation of the hybrid material. Furthermore, the Fe_3O_4@CS−TDI−Titriplex V nanomaterial was used four times with a slight decrease in its catalytic activity.

Introduction

Nanotechnology is defined as the area of science and engineering in which phenomena that occur under specific conditions can be utilized for the design, manufacture, characterisation, and application of materials, devices, structures, and systems at nanoscale dimensions.[1,2] The importance of nanotechnology in both academia and industry has demonstrated the possibility of its use in different fields of science, including chemistry, biomedicine and pharmaceuticals, mechanics, materials science, sensors, safety, adsorbents, and various aspects of technology.[3–17]

Green chemistry and sustainable chemistry, while distinct, are interconnected fields. According to the US Environmental Protection Agency's definition, "green chemistry is the design of chemical products and processes that reduce or eliminate the generation of hazardous substances." The term "sustainable chemistry" has been introduced more recently and

encompasses a multitude of definitions. For example, the Organization for Economic Co-operation and Development defines sustainable chemistry as "a scientific concept that seeks to improve the efficiency with which natural resources are used to meet human needs for chemical products and services." On the other hand, both Anastas and Zimmerman emphasized that green chemistry is a crucial element of sustainable chemistry. Both sustainable and green chemistry have established a steady ground, providing vital design principles for the development of efficient chemical synthesis of complex and high-value molecules.[18–21] Multi-component reaction (MCR) strategies based on sustainable and green chemistry principles have emerged as an attractive and powerful strategy for organic transformations compared to multistep reactions. The MCR strategy allows the formation of several new bonds *via* a one-pot reaction, thereby diminishing the number of reaction and purification stages. This strategy also ensures high selectivity, synthetic convergence, atom economy, simplicity, and synthetic efficiency.[22–24] Different MCRs comprising Strecker, Hantzsch, Biginelli, Mannich, and others are significant transformations for the synthesis of pharmaceutical and biologically active compounds such as acridinediones and 4H-pyrans.[22,25–27] Therefore, MCRs are recently considered a pivotal theme in the

Pharmaceutical and Heterocyclic Compounds Research Laboratory, Department of Chemistry, Iran University of Science and Technology, Tehran, 1684613314, Iran. E-mail: mdekamin@iust.ac.ir

synthesis of numerous libraries of different acyclic and cyclic structures, in particular heterocyclic derivatives.[27–32] However, MCRs often require appropriate mono-, bi- or multi-functional catalytic systems to activate electrophilic, nucleophilic or both of them to afford corresponding products under mild conditions in higher yields and short reaction times.

Due to the drawbacks of previous homogeneous and bulk heterogeneous catalytic systems, including the use of expensive and toxic reagents and solvents for their preparation or operation, as well as the harsh conditions for the recycling and reusability of the catalysts, it is necessary to develop simple methods that employ more efficient and recoverable nano-ordered catalysts under green conditions for the synthesis of desired products of MCRs. Nano-ordered catalysts have several advantages including high turnover number (TON) and turnover frequency (TOF), and long lifetime as well as low toxicity. Hence, effortless optimization of the catalytic activity by simply tuning the catalyst components is underway in both academia and industry.[33–36]

Various supports or additives are used to improve the catalytic performance of nanocatalytic systems, and one of the most important substrates is magnetite (Fe_3O_4).[33,34,37] Magnetic nanoparticles (MNPs) have been considered as an outstanding type of catalyst components because of their good stability, easy synthesis and functionalization, proper surface area and facile separation by a magnetic field as well as low toxicity and price.[38–40] Fe_3O_4 MNPs are an important class of magnetic materials that have been broadly considered for their applications in magnetic resonance imaging (MRI), drug targeting, and hyperthermia treatment as well as pristine catalysts and catalyst supports.[41,42] To improve the biocompatibility and chemical stability of Fe_3O_4 MNPs, they are modified with different materials such as carbon, precious metals, silica, and biopolymers.[43] The basic and applied features of biopolymers address several complex problems related to welfare and well-being as well as sustainable chemistry.[23,44–59] The positive influence of these biopolymers has been intensified by their integration with nanotechnology, which has shown an important development in recent decades.

The application of natural biopolymers as proper supports in the design of new nano-ordered catalytic systems currently attracts considerable attention to produce numerous types of heterogeneous nanomaterials. Biopolymers such as chitosan, cellulose and alginate have been applied as supports in many nano-ordered catalytic systems due to their notable advantages including high natural abundance, biocompatibility, non-toxicity, and biodegradability.[60] In fact, their reactive functional groups including OH, NH_2 and carboxylate make them suitable supports for the preparation of nano-ordered catalysts via the grafting of different building blocks containing appropriate functional groups in their structures.[23,56,61–64]

Biopolymer-based catalytic systems having MNPs in their structures have also been prominent in the field of heterocyclic synthesis via an MCR strategy because of their mild reaction conditions, cost-effectiveness, simple workup, easy recyclability, and modifiable surface properties.[35] Heterocyclic compounds have gained enormous interest and are mainly prepared due to their wide range of biological activities.[65] These compounds including acridine-1,8-dione and 4H-pyran derivatives are used as key scaffolds for the development of many therapeutic agents and play a prominent role in the medicinal chemistry.[66]

Acridine-1,8-dione compounds are a class of heterocyclic compounds with exclusive properties including anticancer, anti-inflammatory, antidiabetic, antimicrobial and antibacterial, and fluorescence activities, which are used in various fields of science such as pharmaceutical, biological, selective fluoride ion chemosensors, and laser dyes (Fig. 1).[67–73]

4H-Pyrans are also abundantly found in the skeleton of natural alkaloids, tocopherols, flavones, and anthocyanins, and they are an important moiety for the discovery of new drug candidates. Furthermore, 4H-pyran derivatives have shown several pharmacological activities such as antiviral, anticancer,[74–76] anti-inflammatory, antitumor, antimicrobial,[77] antiproliferative, anticholinesterase,[78] EPR-1 (effector cell protease receptor-1) antagonists, and MAO (mono-amine oxidase) inhibitors.[79] Among the various structures containing 4H-pyran scaffolds, 2-amino-3-cyano-4H-pyrans have been reported to exhibit highly useful proapoptotic properties for the treatment of a wide range of caner disorders. Several useful examples in this field are shown in (Fig. 2), which are useful for the inhibition of tumor-associated Bcl-2 proteins, inducing apoptosis (programmed cell death), and the ability in the enhancement of mental functions, respectively.[80]

Several homogeneous or heterogeneous catalysts have been reported for the synthesis of acridine-1,8-diones and 2-amino-3-cyano-4H-pyrans.[81,82] Some recent examples include β-cyclodextrin monosulphonic acid,[83] WO_3 nanorods,[84] monodisperse platinum nanoparticles supported with reduced graphene oxide,[85] $ZrCl_4$:$Mg(ClO_4)_2$,[86] Ru-doped hydrotalcite from alcohols,[87] dendritic mesoporous nanosilica functionalized by hexamethylenetetramine,[88] SiO_2–I,[89] betainium lactate ionic liquid,[90] $SnCl_4$-functionalized nano-Fe_3O_4-encapsulated-silica particles,[91] Zn(II) doped and immobilized on functionalized magnetic hydrotalcite,[92] dendrons containing boric acid and 1,3,5-tris(2-hydroxyethyl)isocyanurate covalently attached to silica-coated magnetite,[93] trimesic acid-functionalized chitosan,[71] *Candida parapsilosis* ATCC 7330 biocatalyst,[94] multinuclear [$V^{IV}O$]/[V^VO_2] complexes having triaminoguanidine-based ligands,[95] magnetic nanoparticles functionalized with copper hydroxyproline complexes,[96] copper(II) Schiff-base complex-
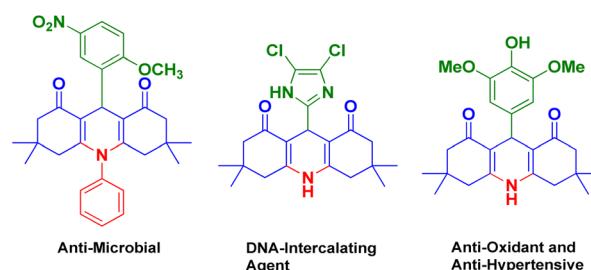

Fig. 1 Selected examples of pharmacologically active compounds based on acridine-1,8-diones.
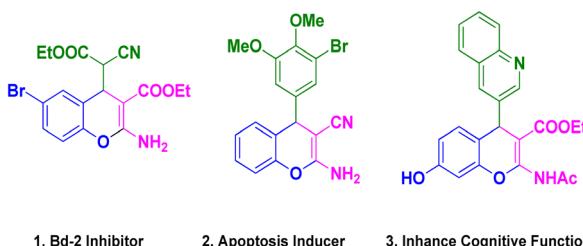
Fig. 2 Selected examples of pharmacologically active compounds based on 4*H*-pyran scaffolds.

modified UiO-66-NH$_2$(Zr) metal–organic frameworks,[97] magnetic reduced graphene oxide aerogel/HKUST-1 (MOF-199),[98] chitosan-EDTA-cellulose network,[27,52] triple superphosphate/titanium tetrachloride,[99] silver nanoparticle-decorated Preyssler-functionalized cellulose biocomposites,[100] redox active organodiselenides,[101] MgMnO$_3$@ZrO$_2$@CoO,[102] Fe$_3$O$_4$@SiO$_2$@NH$_2$@Pd(OAc)$_2$,[103] cysteic acid grafted onto magnetic graphene oxide,[104] (PANI)/Fe$_3$O$_4$/Ag nano-composites,[105] taurine (2-aminoethanesulfonic acid),[106] cyto-chrome c-urea-functionalized dipeptide conjugates,[107] periodic mesoporous organosilica isocyanurate frameworks (PMO-ICS),[15] potassium phthalimide under ball-milling conditions[108] and potassium phthalimide-*N*-oxyl in water under reflux conditions.[24] Although some of the reported methods are practical synthetic procedures, most of them have some limitations, including the use of expensive and hazardous organic

reagents or solvents, extreme reaction conditions, prolonged reaction times, undesirable yields, tedious workup procedures, and high-cost catalyst preparation methods. Therefore, it is necessary to develop simple methods that employ efficient and recoverable catalysts under green conditions for the synthesis of desired acridine-1,8-diones and 2-amino-3-cyano-4*H*-pyran derivatives.[93,109,110]

In continuation of our ongoing efforts towards developing efficient novel homogeneous or heterogenous organocatalytic systems for different organic transformations, in particular MCRs using natural polymers as green catalytic supports,[23,24,26,37,55–57,63,111–114] we designed and prepared a novel Fe$_3$O$_4$@CS–TDI–Titriplex V nanomaterial by grafting diethylenetriaminepentaacetic acid (Titriplex V) to a chitosan backbone using a toluene-2,4-diisocyanate (TDI) linker. The Fe$_3$O$_4$@CS–TDI–Titriplex V nanocomposite (**1**) was used as an efficient solid acid catalyst for the efficient synthesis of acridine-1,8-diones **5** and 2-amino-3-cyano-4*H*-pyrans **7** (Scheme 1).

Results and discussion

The as-prepared magnetic Fe$_3$O$_4$@CS–TDI–Titriplex V nano-material (**1**) was properly characterized using various suitable techniques including Fourier-transform infrared (FTIR) and energy-dispersive X-ray (EDX) spectroscopy, powder X-ray diffraction (XRD), field emission scanning electron micros-copy (FESEM), thermogravimetric and differential thermal analysis (TG-DTA), and vibrating-sample magnetometry (VSM).
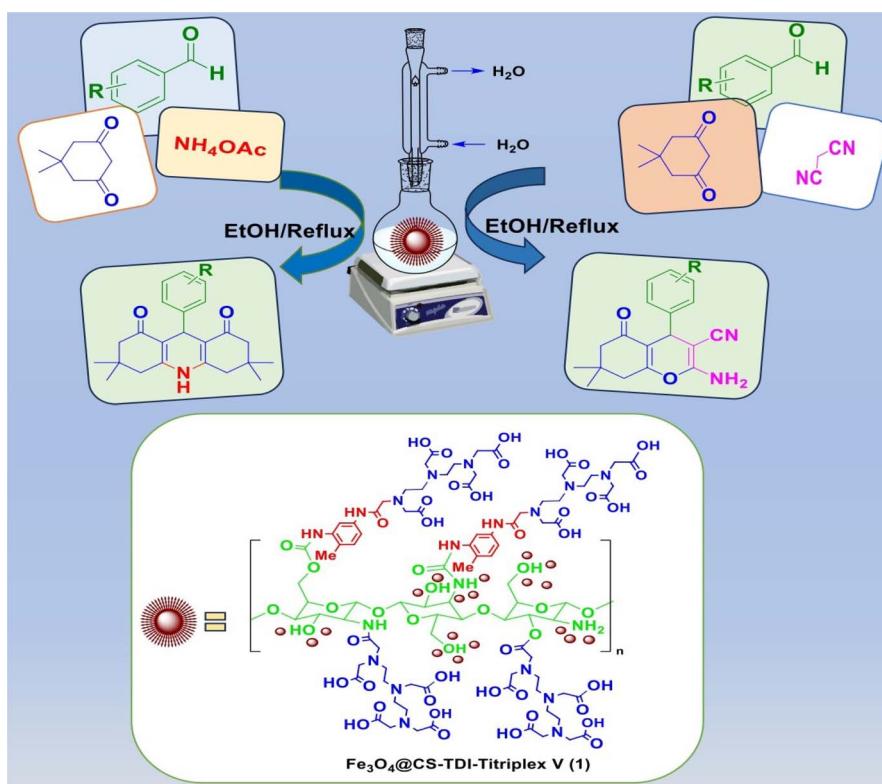

Scheme 1 Synthesis of acridine-1,8-diones and 2-amino-3-cyano-4*H*-pyran derivatives catalyzed by the Fe$_3$O$_4$@CS–TDI–Titriplex V nano-material (**1**).

The process for the preparation of the nano-ordered Fe$_3$O$_4$@CS–TDI–Titriplex V organocatalyst (**1**) is illustrated in Scheme 2. It is well known that when a carboxylic acid functional group reacts with an isocyanate group, the initial product is a mixed acid anhydride, which subsequently undergoes decarboxylation by losing the sp carbon atom of the isocyanate to afford the corresponding *N*-substituted amide. Thus, these two sequential reactions graft Triplex V moiety onto the TDI diisocyanate linker (path A, Scheme 2). In particular, with aromatic isocyanates carrying electron-withdrawing groups (such as the second isocyanate functional group in TDI), this pathway is preferred, leading to the formation of the corresponding amide.[115] Alternatively, it has been approved that another reaction pathway is in competition with the first pathway, which includes the reaction of second acid functional group with the formed mixed acid anhydride before its decarboxylation, producing the anhydride of the used carboxylic acid and the corresponding carbamic acid of the isocyanate (path B, Scheme 2). This pathway's dominance depends on the degree of substitution of the α-carbon of the aliphatic carboxylic acid. For higher substituted
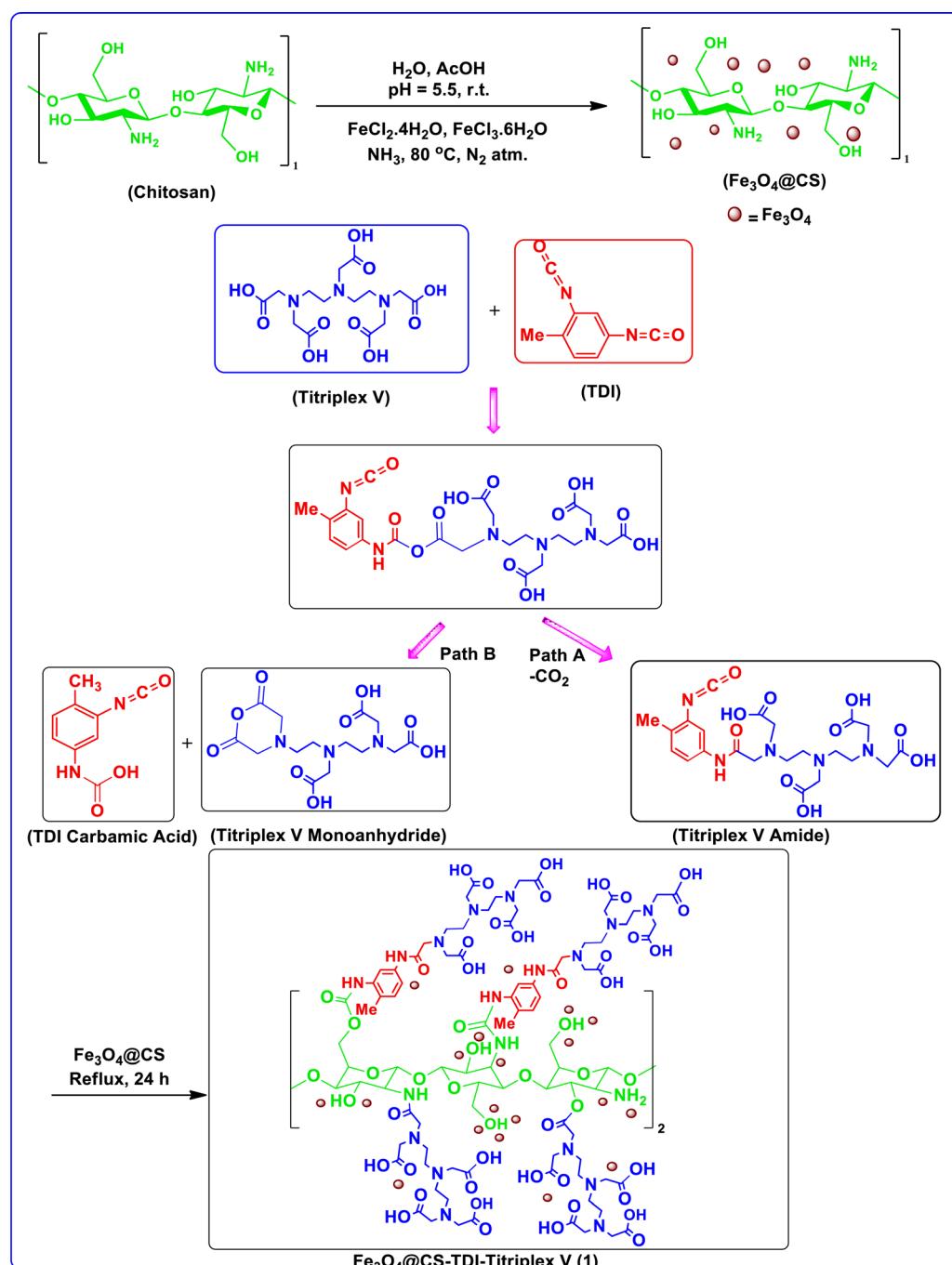
Scheme 2 Schematic preparation and proposed structure for the novel magnetic bio-based Fe$_3$O$_4$@CS–TDI–Titriplex V nanomaterial (**1**).

carboxylic acids such as the used Titriplex V, the second pathway can occur in parallel.[116] The tendency to from acid anhydride is enhanced due to the intermolecular nature of the reaction for Triplex V. As a result, both the first and second pathways generate reactive intermediates that facilitate the smooth grafting of Triplex V onto the chitosan biopolymeric backbone *via* urethane and urea linkages (path A) as well as ester and amide functional groups (path B). These later functional groups can also be formed even through *trans*-amidation or acyl transfer of mono- and possible di-amide produced in path A or di-anhydride in path B.[13,27,52,56,112,114,117,118] Indeed, both di-amide and di-anhydride intermediates may cause cross-linking of the modified chitosan backbone. Hence, the structure proposed in Scheme 2 or its cross-linked form for the magnetic Fe_3O_4@CS–TDI–Titriplex V nanocatalyst **1**, which incorporates both pathways and all of their products, can be obtained.

The FTIR spectra of Fe_3O_4@CS and Fe_3O_4@CS–TDI–Titriplex V organocatalyst (**1**) are illustrated in Fig. 3a–c, respectively. According to Fig. 3, the absorption bands at 529 and 562 cm^{-1}, which are related to the Fe–O vibration can be seen in both spectra of Fe_3O_4@CS (b) and Fe_3O_4@CS–TDI–Titriplex V organocatalyst (**1**, c). Moreover, the observed bands at about 1340 cm^{-1}, 1585 cm^{-1} and 1419 cm^{-1} in the spectrum **3b** are attributed to the NH_2, CO–H, and C–NH bending vibrations of chitosan, respectively. Additionally, three absorption bands at 1645, 1679, 1735, and 1777 cm^{-1} can be seen in the spectrum of Fe_3O_4@CS–TDI–Titriplex V, which are assigned to the corresponding carbonyl functional groups of urea, amide, carbamate, ester and carboxylic acid, respectively. The bands at about 2850–2950 cm^{-1} are ascribed to the stretching vibrations

of aliphatic C–H bonds. The broad band centered at 3250 cm^{-1} is assigned to the stretching vibrations of different O–H and NH bonds of the components existing in the structure of the Fe_3O_4@CS–TDI–Titriplex V organocatalyst (**1**). These results demonstrate the successful grafting of the Titriplex V organocatalyst on the Fe_3O_4@CS backbone support.

The size and morphology of the Fe_3O_4@CS–TDI–Titriplex V nanomaterial (**1**) were investigated by FESEM. The FESEM images showed the changes in the morphology in the pristine chitosan sheets after the grafting of Titriplex V using the toluene-2,4-diisocyanate linker onto a cauliflower-like spherical shape (Fig. 4).[27,37,52,56,62,63,112,113,119] The diameter of the nanoparticles was estimated at about 32–95 nm.

The thermal stability of the Fe_3O_4@CS–TDI–Titriplex V (**1**) organocatalyst was also investigated by the TG-DTA technique. The results are presented in Fig. 5. The thermal stability of the prepared nanomaterial **1** was examined in the temperature range of 50–510 °C. As can be seen, there are three distinct stages of weight loss observed between 220 and 510 °C. The first weight loss occurs between 220 and 280 °C, which can be attributed to the elimination of any physically or chemically sorbed water or organic solvent during the preparation of the sample. The second weight loss (about 13%) was observed between 220 and 370 °C and can be assigned mainly to the decarboxylation of Titriplex V units as well as its complete degradation. The final weight loss occurs at 370–510 °C, which can be correlated with the decomposition of inner moieties including amide, ester, urea or urethane moieties as well as almost volatilization of decomposed chitosan at early stages. According to our previous observations, about 40% degradation of the used commercial chitosan occurs at 200–220 °C.
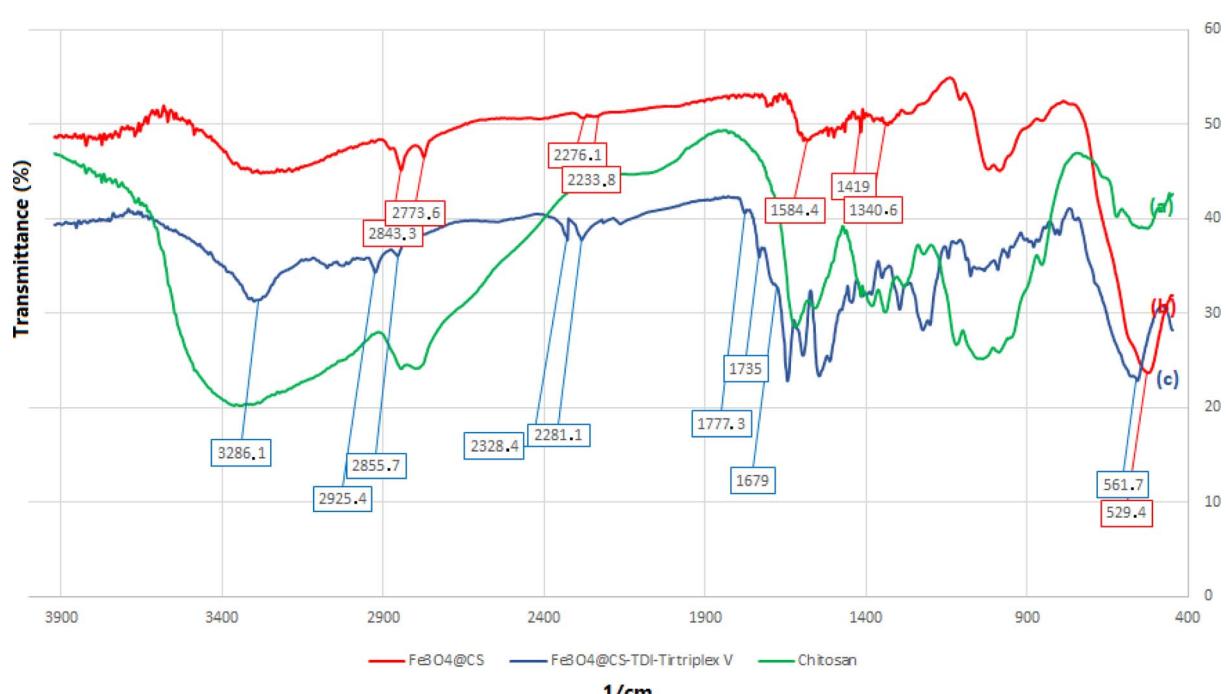

Fig. 3　FTIR spectra of the chitosan (a), Fe_3O_4@CS (b), and Fe_3O_4@CS–TDI–Titriplex V organocatalyst (c).
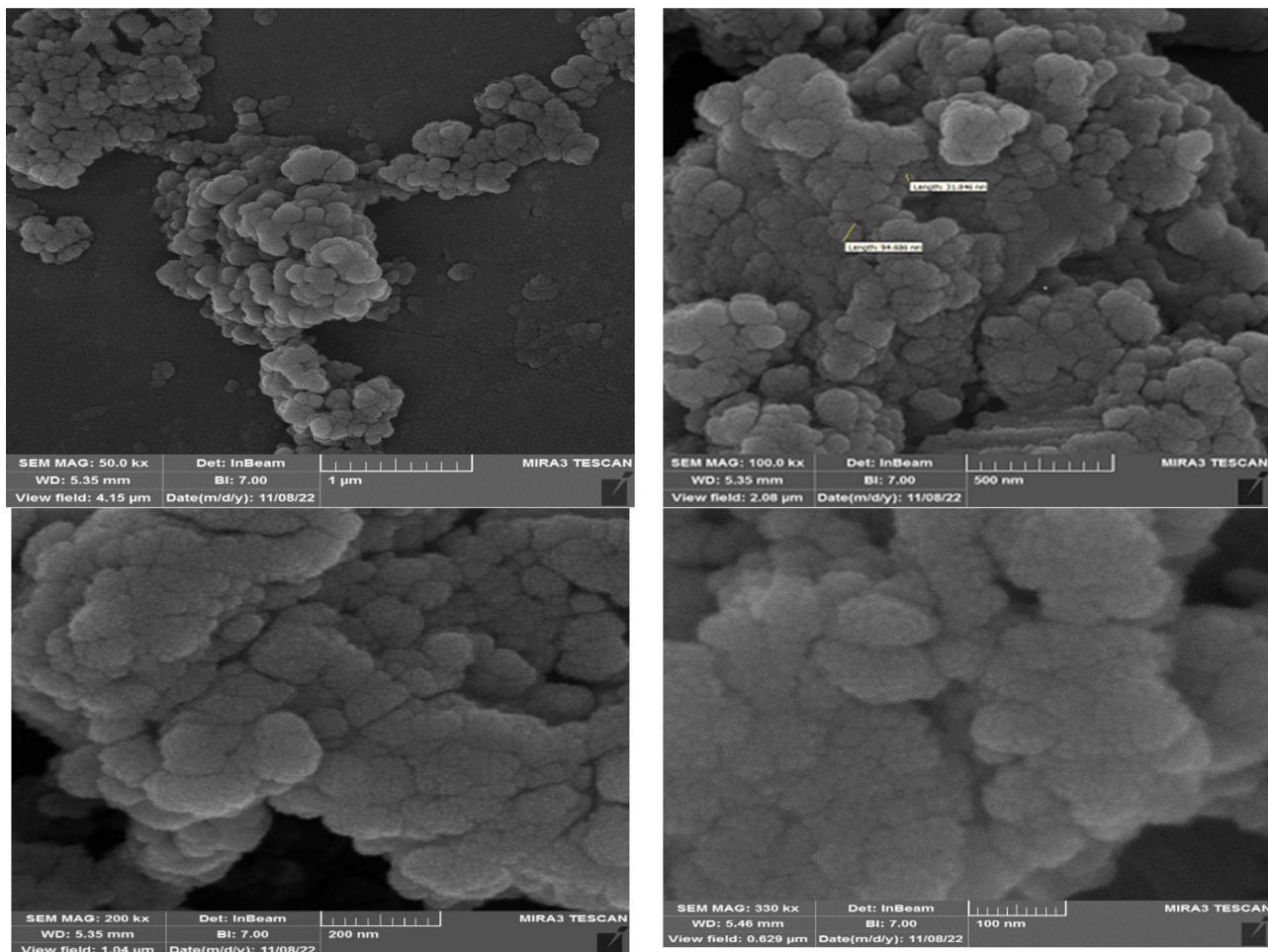
Fig. 4 FESEM images of the Fe_3O_4@CS−TDI−Titriplex V nanomaterial (**1**).
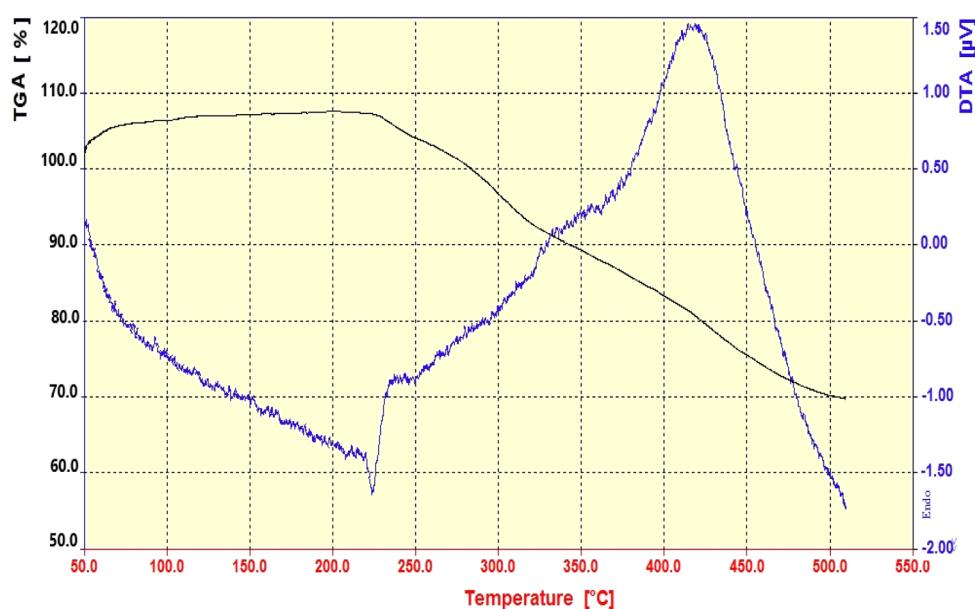
**Fig. 5** TGA and DTA curves of the Fe_3O_4@CS−TDI−Titriplex V nanomaterial (**1**).
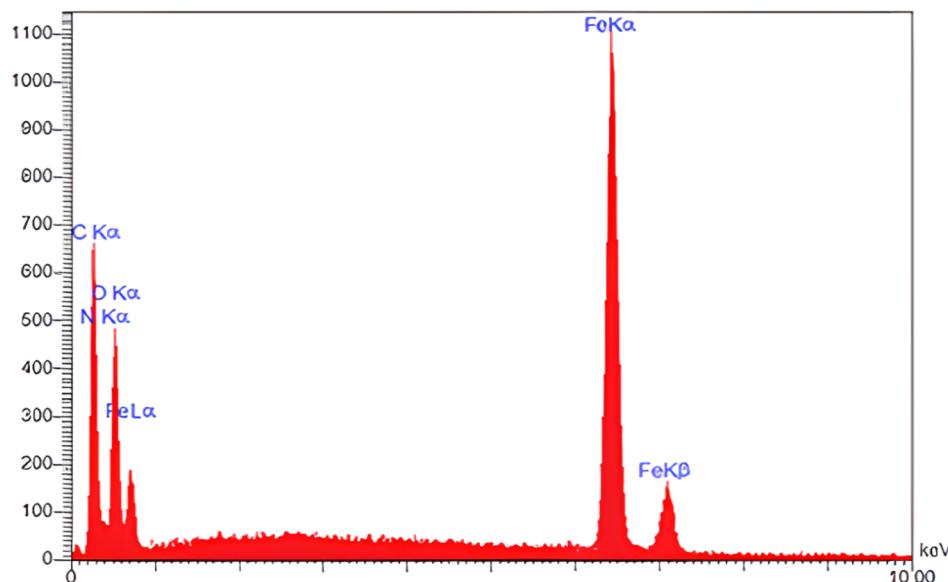
Fig. 6 Energy-dispersive X-ray (EDX) spectrum of the Fe₃O₄@CS–TDI–Titriplex V nanomaterial (**1**).

Therefore, the lower total weight loss (30%), as well as the increase in the thermal stability at a higher temperature in the range of 220–510 °C, demonstrates that the TDI units have been linked on the surface of the chitosan backbone to graft Titriplex V units onto its surface successfully.[52,56,113]

The EDX analysis was also used to confirm the presence of elements in the Fe₃O₄@CS–TDI–Titriplex V nanomaterial (**1**, Fig. 6). It can be implied that the prepared nanomaterial (**1**) contains expected elements including Fe, N, O, and C with mass percentages of 20.76, 16.53, 27.33, and 35.36%, respectively.

Fig. 7 shows the X-ray diffraction (XRD) pattern of the Fe₃O₄@CS–TDI–Titriplex V (**1**) nanocomposite. There are several symmetrical reflections at 2θ, as shown in Fig. 7, which are characteristic of the Fe₃O₄@CS–TDI–Titriplex V (**1**) structure. The matching of the obtained XRD pattern with those of chitosan (JCPDS Card no. 00-039-1894) and Fe₃O₄ (JCPDS Card no. 96-153-2801) confirms the successful preparation of the nanomaterial **1**.

The magnetic properties of the Fe₃O₄@CS–TDI–Titriplex V nanomaterial (**1**) and Fe₃O₄@CS were determined by VSM analysis at room temperature by applying a magnetic field from 10 000 to +10 000 oersted. The results are shown in Fig. 8. According to the obtained curve, the phenomenon of hysteresis was not observed since there is no residual loop in the curve, and this characteristic demonstrates that no accumulation occurs in the presence of a magnetic field. Furthermore, the S-shaped curve for the Fe₃O₄@CS–TDI–Titriplex V nanomaterial (**1**) and Fe₃O₄@CS exhibits excellent paramagnetic behaviors without any hindrance or reluctance. The saturation magnetic moments of the Fe₃O₄@CS–TDI–Titriplex V nanomaterial (**1**) and Fe₃O₄@CS were 50.334743 and 36.300318 emu g⁻¹, respectively, which are lower than the magnetization of Fe₃O₄. This can be explained by the fact that by coating Fe₃O₄ nanoparticles with diamagnetic chitosan, TDI linkers and Titriplex V

units, their magnetization was reduced, but the grafting process of Titriplex V did not affect the magnetization very much and allows its convenient separation by implying an external magnetic field.

Finally, the acidity of the Fe₃O₄@CS–TDI–Titriplex V nanomaterial (**1**) was calculated by a back titration method.[27,52] According to the obtained results, the concentration of proton, [H⁺], on the surface of the Fe₃O₄@CS–TDI–Titriplex V nanomaterial was calculated to be about 1.47 mmol g⁻¹.

Optimization of the catalytic activity of Fe₃O₄@CS–TDI–Titriplex V nanomaterial (1) for the Hantzsch synthesis of acridine-1,8-diones 5a–j

In this section, the efficacy of the Fe₃O₄@CS–TDI–Titriplex V nanomaterial (**1**) was examined in the model reaction for the synthesis of acridine-1,8-dione derivatives. The pseudo-four-component condensation of dimedone (**2**, 2.0 mmol), 4-chlorobenzaldehyde (**3a**, 1.0 mmol), and ammonium acetate (**4**, 1.2 mmol) in the presence of the Fe₃O₄@CS–TDI–Titriplex V nanomaterial (**1**) was investigated as a model reaction. The results are summarized in Table 1. The effects of several key factors such as catalyst loading, reaction temperature, solvent and reaction time on the yield of desired product 9-(4-chlorophenyl)-3,3,6,6-tetramethyl-3,4,6,7,9,10-hexahydroacridine-1,8(2H,5H)-dione (**5a**) were systemically investigated. In the absence of catalyst **1**, the reaction did not proceed even after 120 min in EtOH (entry 1, Table 1). The reaction yield was found to be only 50% when 20 mg of the Fe₃O₄@CS–TDI–Titriplex V nanomaterial (**1**) was used under solvent-free conditions at 120 °C after 80 min (entry 2, Table 1). The model reaction was further investigated in several solvents including EtOH, H₂O, MeOH, THF, CH₃CN, and EtOAc under the same catalyst loading (entries 3–8, Table 1), but the best result was obtained in EtOH under reflux conditions after 30 min (entry 4, Table 1).
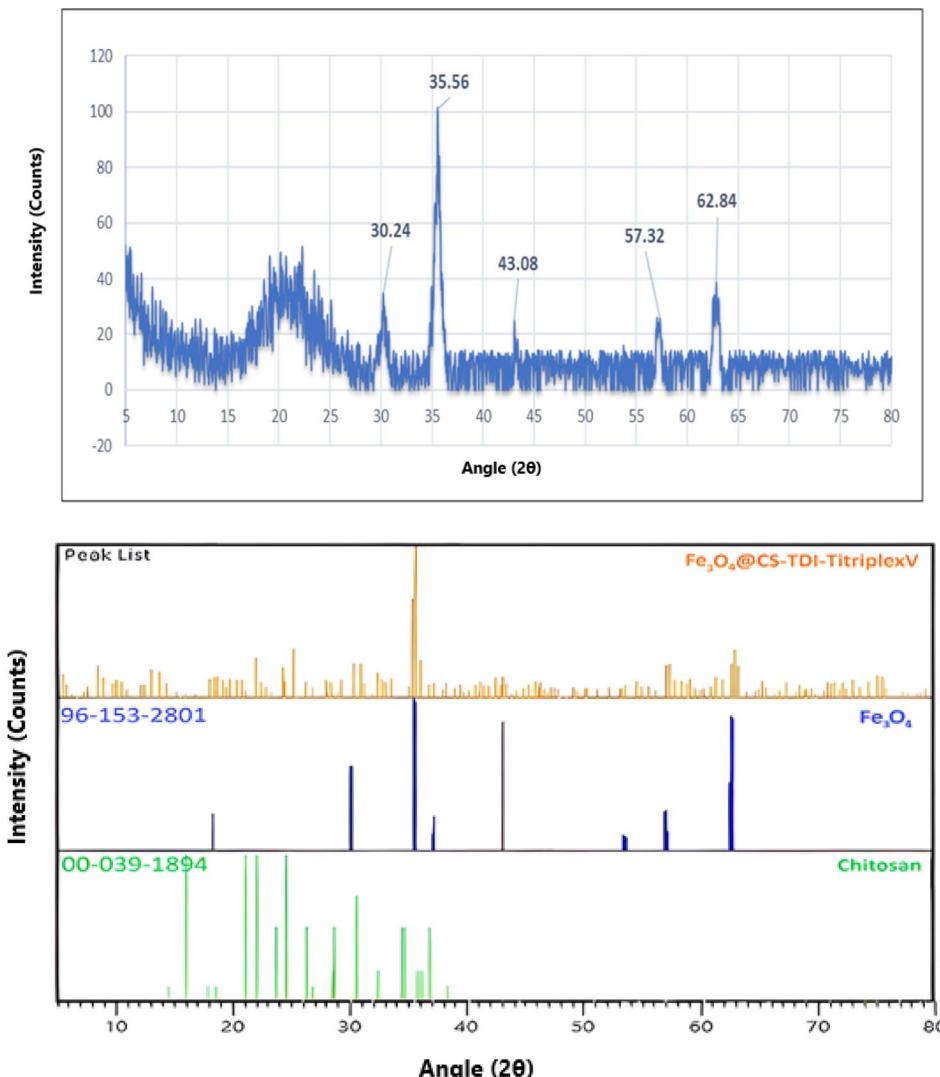
Fig. 7 Powder X-ray diffraction (XRD) pattern of the Fe_3O_4@CS–TDI–Titriplex V nanomaterial (**1**) in the wide angle region and its comparison with the X'pert high-score data.

Moreover, moderate yields of the desired product **5a** were obtained at room temperature for the model reaction in both water and EtOH (entries 9, 10, Table 1). Furthermore, 15 and 10 mg catalyst **1** loadings in EtOH under reflux conditions afforded 82% and 67% of the desired product **5a** after 30 min, respectively (entries 11, 12, Table 1). In our hands, commercial CS with medium MW, Titriplex V and Fe_3O_4@CS with 20 mg loading in EtOH under reflux conditions afforded 39, 78 and 63% of the desired product **5a** after 30 min compared to the Fe_3O_4@CS–TDI–Titriplex V nanomaterial (**1**) (entries 4, 13–15, Table 1). The obtained data clearly show the synergistic effects of the Fe_3O_4@CS–TDI–Titriplex V component on its catalytic activity. Therefore, the optimized conditions for the model reaction in the synthesis of acridine-1,8-dione derivatives were 20 mg catalyst loading in EtOH under reflux conditions. These optimized conditions were developed for other aromatic aldehydes **3b–j** for the synthesis of the desired products **5a–j**. The results are summarized in Table 2.

Optimization of the catalytic activity of Fe_3O_4@CS–TDI–Titriplex V nanomaterial (1) for the synthesis of 2-amino-3-cyano-4H-pyrans 7a–j

The excellent catalytic activity of the Fe_3O_4@CS–TDI–Titriplex V nanomaterial (**1**) in the synthesis of acridine-1,8-diones encouraged us to explore this useful nano-ordered organo-catalyst **1** for the synthesis of highly functionalized bioactive 2-amino-3-cyano-4H-pyran derivatives **7**. It was found that 2-amino-4-(4-chlorophenyl)-7,7-dimethyl-5-oxo-5,6,7,8-tetrahydro-4H-pyran-3-carbonitrile (**7a**) can also be prepared via one-pot condensation of dimedone (1.0 mmol, **2**), 4-hydroxybenzaldehyde (1.0 mmol, **3a**), and malononitrile (1.0 mmol, **6**), as a model reaction, in the presence of catalytic amounts of Fe_3O_4@CS–TDI–Titriplex V nanomaterial (**1**). The optimization results are summarized in Table 3. Initial experiments indicated that in the absence of organocatalyst **1**, the desired product **7a** was not obtained even after 120 min (entry 1, Table 3). The isolated yield of the model reaction was a mere 60% when 20 mg
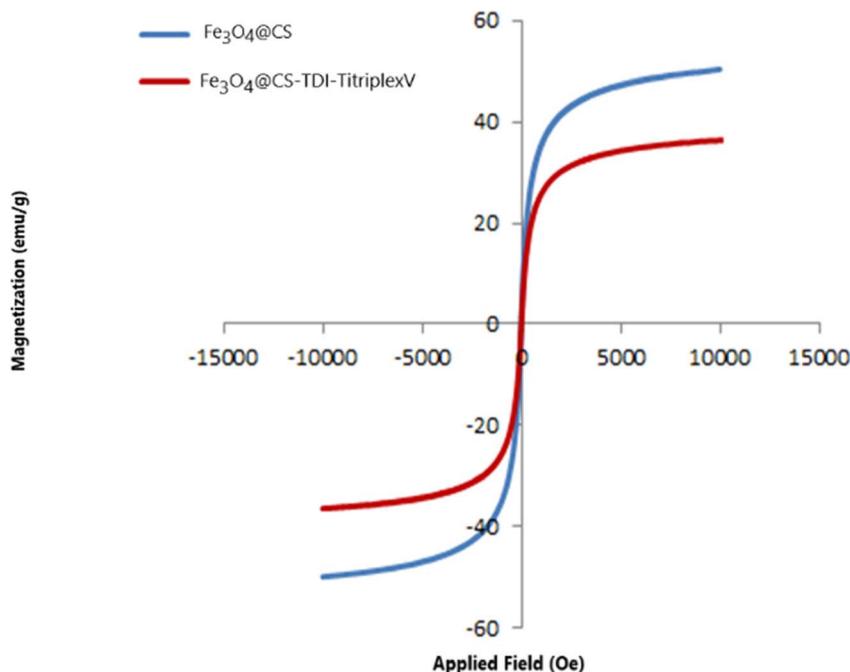
Fig. 8 VSM plots of Fe_3O_4@CS–TDI–Titriplex V nanomaterial (**1**) (red) and Fe_3O_4@CS (blue).
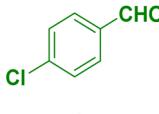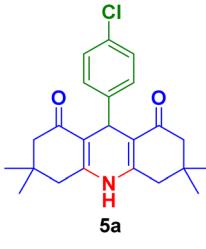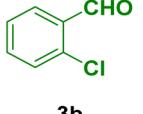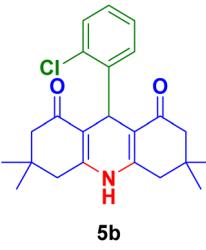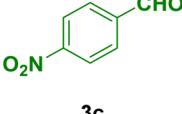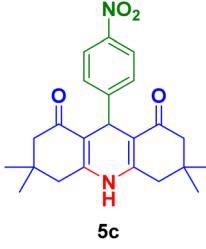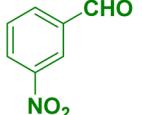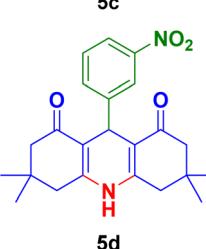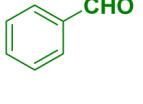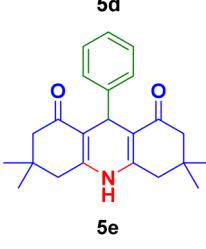
Table 1 Optimization of the conditions in the reaction of dimedone (**2**), 4-chlorobenzaldehyde (**3a**), and ammonium acetate (**4**) under different conditions[a]
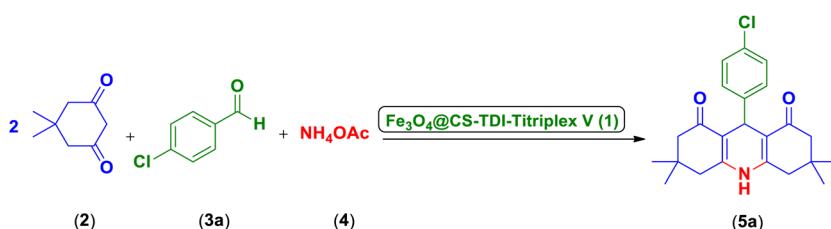
Entry	Catalyst (mg)	Solvent	Temp. (°C)	Time (min)	Yield[b] (%)
1	—	EtOH	Reflux	120	Trace
2	20	Solvent-free	120	80	50
3	20	H_2O	Reflux	60	70
4	**20**	**EtOH**	**Reflux**	**30**	**90**
5	20	EtOAc	Reflux	60	80
6	20	CH_3CN	Reflux	60	60
7	20	THF	Reflux	60	74
8	20	MeOH	Reflux	30	80
9	20	H_2O	Room temperature	80	65
10	20	EtOH	Room temperature	50	70
11	15	EtOH	Reflux	30	82
12	10	EtOH	Reflux	30	67
13	20[c]	EtOH	Reflux	30	39
14	20[d]	EtOH	Reflux	30	78
15	20[e]	EtOH	Reflux	30	63

[a] Reaction conditions: dimedone (**2**, 2.0 mmol), 4-chlorobenzaldehyde (**3a**, 1.0 mmol), ammonium acetate (**4**, 1.2 mmol), Fe_3O_4@CS–TDI–Titriplex V (**1**) and solvent (2 mL) unless otherwise stated. [b] Isolated yields. [c] Commercial CS with medium MW was used. [d] Titriplex V was used. [e] Fe_3O_4@CS was used.

Table 2 Scope of the synthesis of 9-(aryl)-3,3,6,6-tetramethyl-3,4,6,7,9,10-hexahydroacridine-1,8(2H,5H)-dione derivatives **5a–j** catalyzed by the Fe$_3$O$_4$@CS–TDI–Titriplex V organocatalyst (**1**) via a pseudo-four-component reaction strategy[a]

Entry	Aldehyde 3	Product 5	Time (min)	Yield[b] (%)	M.P. (°C) observed	M.P. (°C) (reported)
1	3a	5a	30	90	300<	243–245 (ref. 120)
2	3b	5b	35	90	261–263	263–264 (ref. 121)
3	3c	5c	40	80	300	302–304 (ref. 122)
4	3d	5d	40	82	293–295	294–296 (ref. 123)
5	3e	5e	30	90	275–276	272 (ref. 27)
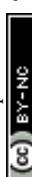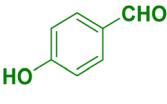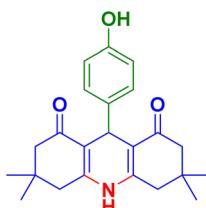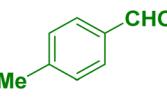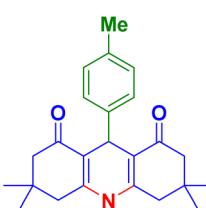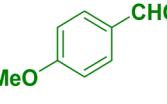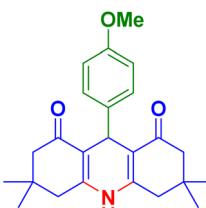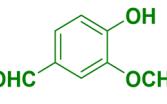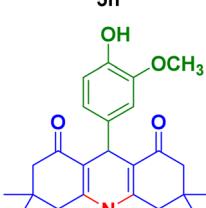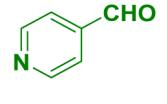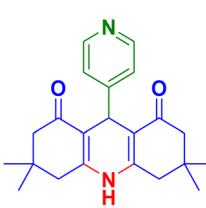
Table 2 (*Contd.*)

Entry	Aldehyde 3	Product 5	Time (min)	Yield[b] (%)	M.P. (°C) observed	M.P. (°C) (reported)
6	3f	5f	40	90	300<	300< (ref. 124)
7	3g	5g	50	80	300<	300< (ref. 90)
8	3h	5h	50	80	276–278	278–280 (ref. 125)
9	3i	5i	45	82	297	295–298 (ref. 126)
10	3j	5j	45	90	245	248–250 (ref. 90)

[a] Reaction conditions: dimedone (**2**, 2.0 mmol), aldehyde (**3**, 1.0 mmol), ammonium acetate (**4**, 1.2 mmol), Fe₃O₄@CS–TDI–Titriplex V (**1**, 20 mg) in EtOH (96%, 2 mL). [b] Isolated yields.
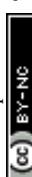
Table 3 Optimization of the conditions in the reaction of dimedone (2), 4-chlorobenzaldehyde (3a), and malononitrile (6) under different conditions[a]
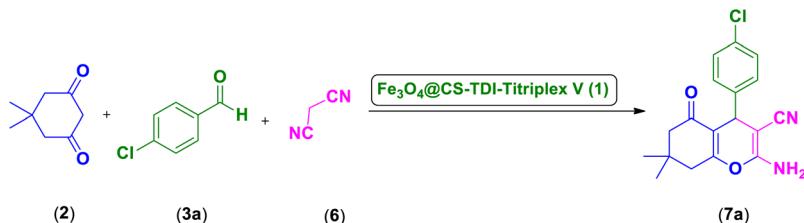
Entry	Catalyst (mg)	Solvent	Temp. (°C)	Time (min)	Yield[b] (%)
1	—	EtOH	Reflux	120	Trace
2	20	Solvent-free	120	120	60
3	20	H$_2$O	Reflux	40	88
4	**20**	**EtOH**	**Reflux**	**15**	**95**
5	20	EtOAc	Reflux	60	80
6	20	CH$_3$CN	Reflux	25	90
7	20	THF	Reflux	35	70
8	20	MeOH	Reflux	30	90
9	20	H$_2$O	Room temperature	60	80
10	20	EtOH	Room temperature	60	85
11	20[c]	EtOH	Reflux	15	41
12	20[d]	EtOH	Reflux	15	81
13	20[e]	EtOH	Reflux	30	45

[a] Reaction conditions: dimedone (2, 1.0 mmol), 4-chlorobenzaldehyde (3a, 1.0 mmol), malononitrile (6, 1.1 mmol), Fe$_3$O$_4$@CS–TDI–Titriplex V (1) and solvent (2 mL) unless otherwise stated. [b] Isolated yields. [c] Commercial CS with medium was used. [d] Titriplex V was used. [e] Fe$_3$O$_4$@CS was used.

loading of the Fe$_3$O$_4$@CS–TDI–Titriplex V nanomaterial (1) was used under solvent-free conditions at 120 °C for 80 min (entry 2, Table 2). Surprisingly, the desired product 7a was obtained in 88% and 92% isolated yields when the model reaction was performed in water and EtOH under reflux conditions (entries 3–4, Table 2). However, screening the reaction conditions in other solvents under reflux conditions or at room temperature afforded lower yields of the desired product 7a (entries 5 10, Table 2). Again, commercial CS with medium MW, Titriplex V and Fe$_3$O$_4$@CS with 20 mg loading in EtOH under reflux conditions afforded 41, 81 and 45% of the desired product 7a after 15 min, respectively, compared to the Fe$_3$O$_4$@CS–TDI–Titriplex V nanomaterial (1) (entries 4, 11–13, Table 2). These outstanding findings prompted us for the synthesis of various 2-amino-3-cyano-4H-pyran derivatives 7a–j under optimized reaction conditions in high to excellent yields and short reaction times. The results are summarized in Table 4.

In general, high to excellent yields of the desired products acridine-1,8-diones 5 as well as 2-amino-3-cyano-4H-pyrans 7 were obtained in EtOH, a green solvent, under reflux conditions in short reaction times. Furthermore, carbocyclic and heterocyclic aldehydes bearing electron-withdrawing substituents including Cl and NO$_2$ (3a–d) or 4-pyridyl (3i) afforded higher yields in shorter reaction times than that of benzaldehyde (3e) or other aldehydes having electron-donating groups such as OH, MeO or Me (3f–i). All these data imply that Knoevenagel condensation is the rate-determining step in both multi-

component reactions for the synthesis of acridine-1,8-diones 5 as well as 2-amino-3-cyano-4H-pyrans 7 in the presence of the Fe$_3$O$_4$@CS–TDI–Titriplex V nanocatalyst (1) (Scheme 3 and 4).

Proposed mechanisms for the synthesis of acridine-1,8-diones 5 and 2-amino-3-cyano-4H-pyrans 7 in the presence of the Fe$_3$O$_4$@CS–TDI–Titriplex V nanocatalyst (1)

According to the obtained results, the following mechanism can be proposed for the Hantzsch synthesis of acridine-1,8-diones 5 via the MCR pathway (Scheme 3). In the first step, the catalyst 1 activates the carbonyl functional group of aldehydes 3, which is reacted with one equivalent of dimedone in its enol form 2′ to form intermediates (I) and (II) subsequently by the Knoevenagel condensation. The formed Knoevenagel intermediate (II) is activated again with catalyst 1 and reacts with the second equivalent of dimedone in its enol form 2′ to produce intermediate (III) via the Michael addition. By adding the amine, obtained from NH$_4$OAc (4), to the activated intermediate (III), the iminium salt of intermediate (IV) was obtained. After conversion to the stable enamine form (V), its carbonyl group is activated again by catalyst 1 and after second amine attack and hetero-annulation, the intermediate (VI) is converted to the desired products 5 by elimination of a water molecule and the catalyst is recycled as well. Furthermore, all the above-mentioned steps are competitively catalyzed via hydrogen bonding by plenty of hydrogen donors on

Table 4 Scope of the synthesis of 2-amino-4-(4-aryl)-7,7-dimethyl-5-oxo-5,6,7,8-tetrahydro-4H-pyran-3-carbonitrile derivatives **7a–j** catalyzed by the Fe_3O_4@CS–TDI–Titriplex V organocatalyst (**1**) via a three-component reaction strategy[a]
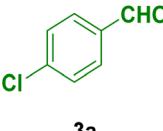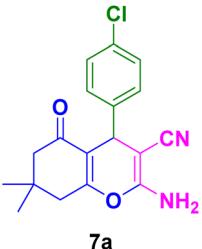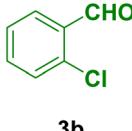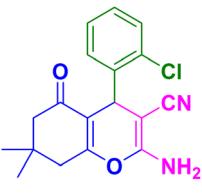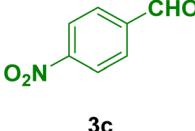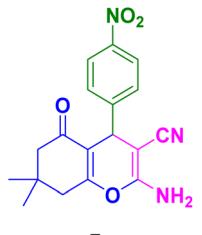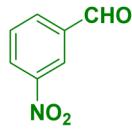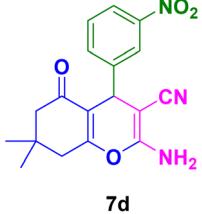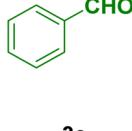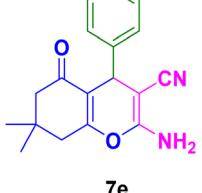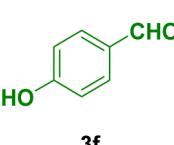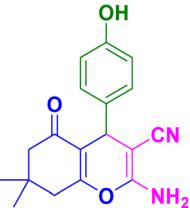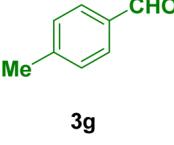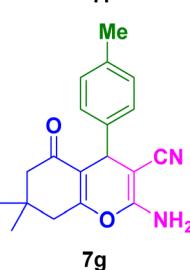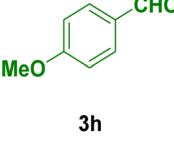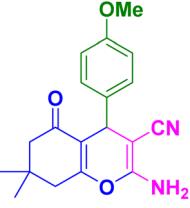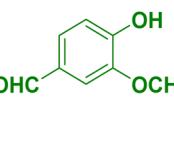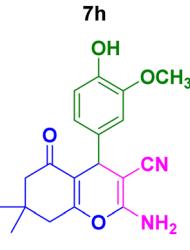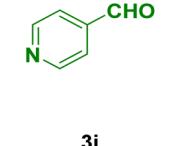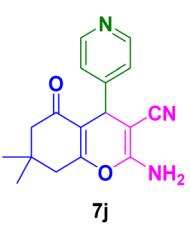

Entry	Aldehyde **3**	Product **7**	Time (min)	Yield[b] (%)	M.P. (°C) observed	M.P. (°C) (reported)
1	**3a**	**7a**	15	95	212	212–214 (ref. 127)
2	**3b**	**7b**	15	90	210–212	210–212 (ref. 128)
3	**3c**	**7c**	20	90	234–236	234–235 (ref. 103)
4	**3d**	**7d**	20	89	233–235	236–238 (ref. 129)
5	**3e**	**7e**	15	90	228–230	228–230 (ref. 130)

Table 4 (*Contd.*)

Entry	Aldehyde 3	Product 7	Time (min)	Yield[b] (%)	M.P. (°C) observed	M.P. (°C) (reported)
6	3f	7f	30	90	202–204	203–205 (ref. 131)
7	3g	7g	30	89	219–221	219–221 (ref. 132)
8	3h	7h	35	80	202–204	202–204 (ref. 84)
9	3i	7i	30	85	230–231	230–231 (ref. 133)
10	3j	7j	40	84	263–265	260–262 (ref. 134)

[a] Reaction conditions: dimedone (2, 2.0 mmol), aldehyde (3, 1.0 mmol), malononitrile (6, 1.1 mmol), Fe$_3$O$_4$@CS–TDI–Titriplex V (1, 20 mg) in EtOH (96%, 2 mL). [b] Isolated yields.
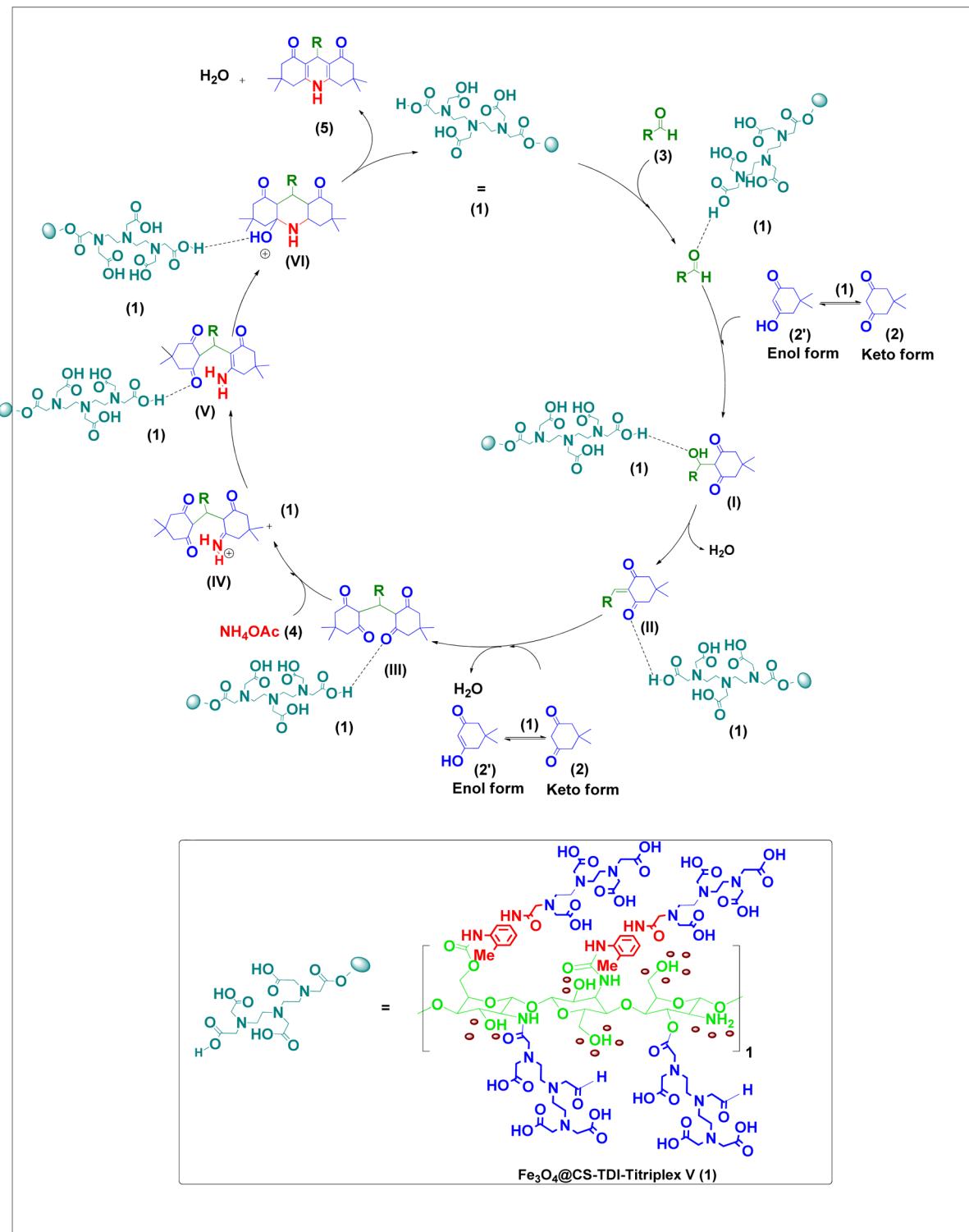
Scheme 3 Plausible mechanism for the Hantzsch pseudo-four-component synthesis of acridine-1,8-diones **5** from different dimedone (**2**), aldehydes **3a–j** and NH₄OAc (**4**) catalyzed by the Fe₃O₄@CS–TDI–Titriplex V nanocatalyst (**1**).

the surface of the organocatalyst **1** parallel to the proton transfer by the carboxylic acid groups of the catalyst.

Moreover, the proposed mechanism for the synthesis of 2-amino-3-cyano-4*H*-pyran derivatives catalyzed by the Fe₃O₄@CS–TDI–Titriplex V organocatalyst (**1**) is shown in

Scheme 4. As can be seen, Fe₃O₄@CS–TDI–Titriplex V (**1**) acts as a Brønsted acid and activates the carbonyl group of aldehydes **3** by increasing its electrophilicity. Therefore, aldehydes **3** and malononitrile (**6**) are condensed together *via* the Knoevenagel condensation to afford intermediate **VII**, and after elimination
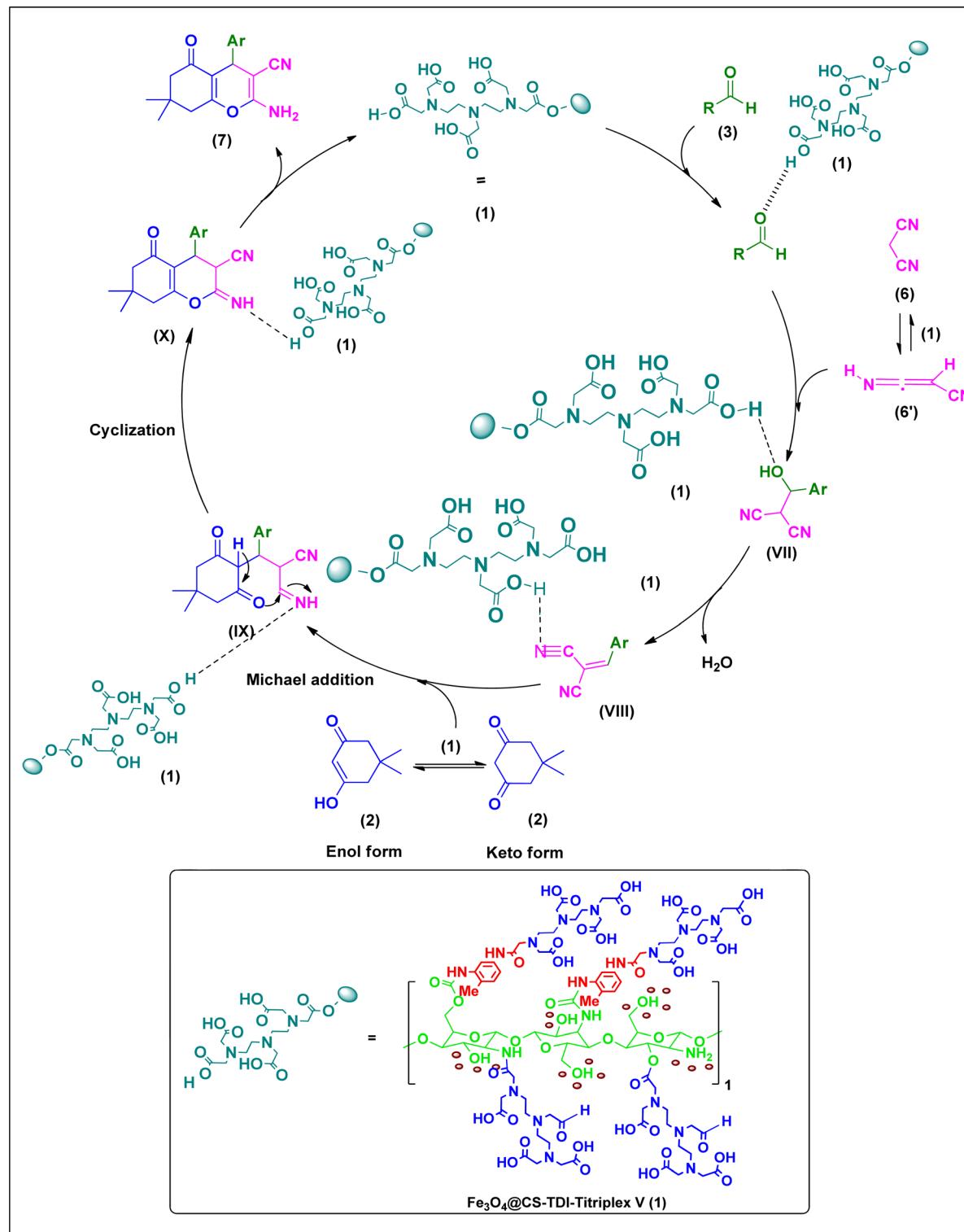
Scheme 4 Plausible mechanism for the three-component synthesis of 2-amino-3-cyano-4H-pyrans **7** from dimedone (**2**), different aldehydes **3** and malononitrile (**6**) catalyzed by the Fe₃O₄@CS–TDI–Titriplex V nanocatalyst (**1**).

of a water molecule, the Knoevenagel intermediate (**VIII**) is formed. Then, this intermediate (**VIII**) acts as a Michael acceptor to combine with the dimedone as an active enolizable C–H acidic compound and affords the corresponding open-chain intermediate (**IX**). Finally, the intramolecular cyclization of the intermediate (**IX**) forms the imine intermediate (**X**), which can afford the desired product **7** upon its tautomerization, and liberates the catalyst for the next run.

The recyclability and reusability of the heterogenous nano-ordered catalyst is a vital factor in the design of more efficient
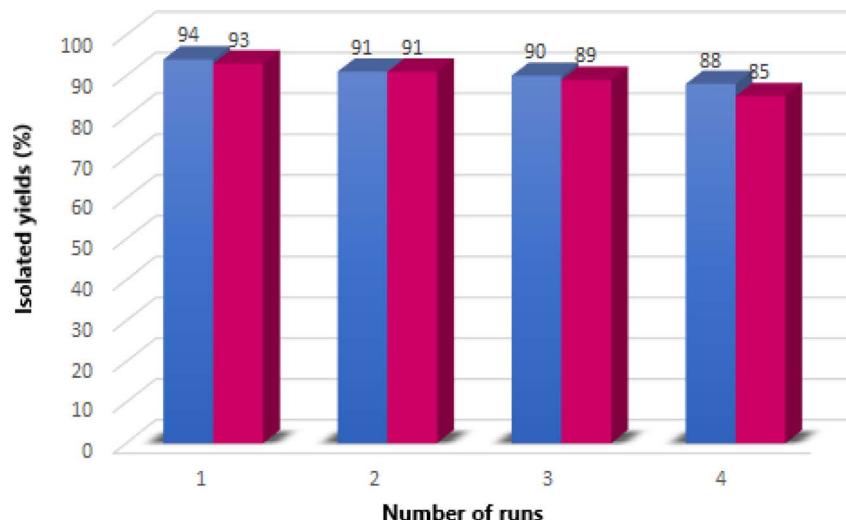
Fig. 9   Reusability of the heterogeneous Fe_3O_4@CS−TDI−Titriplex V nanocatalyst (**1**) for the synthesis of **5a** (blue charts) and **7a** (red charts).
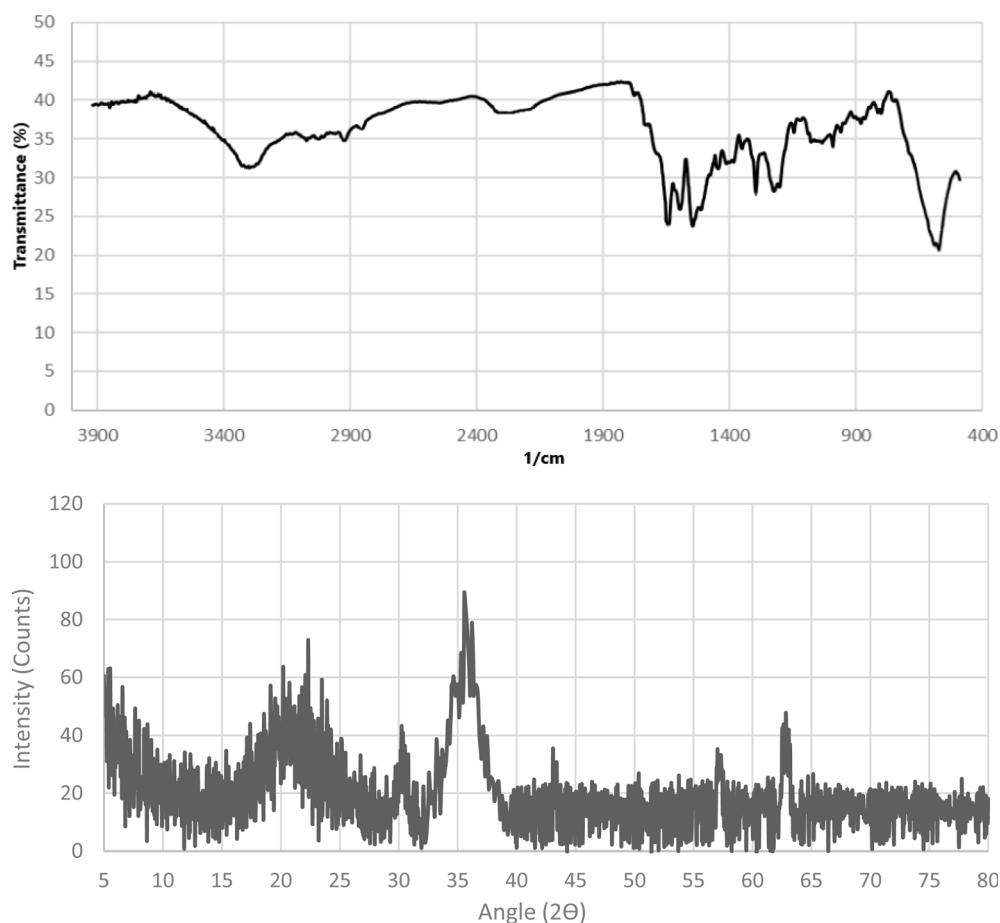
Fig. 10   FTIR spectra and XRD pattern of the recovered Fe_3O_4@CS−TDI−Titriplex V nanocatalyst (**1**) after recovery from the fourth cycle of the model reactions.

catalytic systems. Hence, the reusability of the Fe_3O_4@CS−TDI−Titriplex V nanocatalyst (**1**) was also examined for the two model reactions in other parts of our study. The results are summarized in Fig. 9. In our work, the fresh Fe_3O_4@CS−TDI−Titriplex V nanocatalyst (**1**) was easily separated after the completion of the reaction showed by thin layer

Table 5 Comparative synthesis of compounds **5a** and **7a** using the reported homogeneous or heterogeneous catalysts *versus* the present method

Entry	Catalyst	Product	Catalyst loading	Reaction conditions	Time (min)	Yield (%)	Ref.
1	β-Cyclodextrin monosulphonic acid	**5a**	30 mg	H_2O-60 °C	120	91	83
2	Ascorbic acid	**5a**	8.8 mg	Solvent-free/80 °C	180	89	135
3	$SnCl_4$-functionalized nano-Fe_3O_4 encapsulated-silica	**5a**	25 mg	EtOH/reflux	15	93	91
4	TiO_2-coated magnetite nanoparticle-supported sulfonic acid	**5a**	10 mg	Solvent-free/110 °C	40	95	136
5	**Fe_3O_4@CS–TDI–Titriplex V**	**5a**	**20 mg**	**EtOH/reflux**	**30**	**90**	**This work**
6	4-(Dimethylamino)pyridine (DMAP)	**7a**	24 mg	EtOH/reflux	15	94	137
7	Sodium alginate	**7a**	22 mg	EtOH/reflux	50	93	26
8	Fe_3O_4–chitosan	**7a**	30 mol%	Ultrasound irradiation at 50 °C	20	99	60
9	Triethylbenzylammonium chloride (TEBA)	**7a**	100 mol% (228 mg)	H_2O-90 °C	420	94	138
10	**Fe_3O_4@CS–TDI–Titriplex V**	**7a**	**20 mg**	**EtOH/reflux**	**15**	**95**	**This work**

chromatography (TLC). Indeed, an appropriate amount of EtOH was added to the reaction mixture to dissolve the precipitates of the products by heating, and the magnetic nanocatalyst **1** was subsequently separated using an external magnet. The recycled catalyst **1** was suspended in acetone (1.0 mL), stirred for 30 minutes, and then filtered off. The recycled Fe_3O_4@CS–TDI–Titriplex V nanocatalyst (**1**) was dried in an oven at 60 °C for 1.5 h to be used in the next run of the model reactions under the same conditions. This process was repeated for four cycles. The obtained results demonstrate that the Fe_3O_4@CS–TDI–Titriplex V nanocatalyst (**1**) is stable enough and effective under optimized conditions to promote the studied MCRs for at least four runs. Both FTIR spectra and XRD pattern of the recovered Fe_3O_4@CS–TDI–Titriplex V nanocatalyst after recovery from the fourth cycle of the model reactions demonstrate that its structure is very similar to the fresh one and confirms its stability under optimized conditions (Fig. 10). Furthermore, the heterogeneous nature of the catalyst was studied by a hot filtration test. In this part of our study, the model reactions for the synthesis of **5a** and **7a** were heated under optimized conditions for 15 and 7.5 min, respectively. Then, the Fe_3O_4@CS–TDI–Titriplex V nanocatalyst (**1**) was separated from the reaction mixtures by using an external magnet and the obtained mixtures were heated in EtOH under solvent-free conditions for further 15 and 7.5 min, respectively. Interestingly, lower yields of the desired products **5a** (55%) and **7a** (62%) were isolated at the end of both model reactions. These data confirm that the Fe_3O_4@CS–TDI–Titriplex V nanocatalyst (**1**) maintains a heterogeneous nature, and leaching of its components to the reaction mixture does not occur under optimized conditions.

Finally, to demonstrate the capability and efficiency of the present protocols in the synthesis of different acridine-1,8-diones and 2-amino-3-cyano-4*H*-pyran derivatives, they were compared with some of the published procedures and previously reported ones. The results summarized in Table 5 clearly show that the present protocols for both reactions are indeed superior to several of the others in terms of product yield, catalyst loading, temperature and reaction time.

Experimental section

Reagents and instruments

All the chemicals were purchased from Merck or Aldrich companies and used without further purification, except for benzaldehyde, which was used as a freshly distilled sample. Chitosan (MW = 100 000–300 000 Da) was purchased from Acros Organics. Melting points were determined using an Electrothermal 9100 apparatus, and are uncorrected. The characterization of the Fe_3O_4@CS–TDI–Titriplex V nanocatalyst (**1**) was carried out using FESEM TESCAN-MIRA3, EDX Numerix DXP-X10P, Shimadzu FT-IR-8400S, and TGA Bahr Company STA 504. Analytical thin-layer chromatography (TLC) was performed using Merck 0.2 mm silica gel 60F-254 Al-plates. FTIR spectra were recorded using a Shimadzu FT IR-8400S spectrometer with KBr pellets. ^1H NMR (500 MHz) spectra were recorded using a Bruker DRX-500 Advance spectrometer in DMSO-d_6 as the solvent at ambient temperature. All yields refer to the isolated products. All the products are known compounds and were identified by comparison of their physical, spectroscopic and analytical data with the authentic samples.

General procedure for the preparation of the magnetic Fe_3O_4@CS nanoparticles

Fe_3O_4 nanoparticles were prepared by chemical co-precipitation of $FeCl_3 \cdot 6H_2O$ and $FeCl_2 \cdot 4H_2O$ ions with a molar ratio of 2/1, in the presence of chitosan, followed by hydrothermal treatment. Chitosan is only soluble in acidic aqueous solutions at pH values lower than 6.5. Then, 0.20 g of chitosan was dissolved in an AcOH solution (0.05 M, 10.0 mL), to which $FeCl_3 \cdot 6H_2O$ (0.30 g) and $FeCl_2 \cdot 4H_2O$ (0.15 g) were added. The resulting solution was mechanically stirred in a N_2 atmosphere at 80 °C for 6 h. Consequently, an ammonia solution (25%, 5.0 mL) was injected dropwise into the reaction mixture with constant stirring. After 30 min, the mixture was cooled to room temperature, and

chitosan nanomagnetic particles were separated by using an external magnet, washed first with distilled water to reach the neutral pH and then with EtOH (96%, 5.0 mL), and finally dried under vacuum at room temperature for 12 h to obtain a Fe_3O_4@CS black solid material.

General procedure for the preparation of the Fe_3O_4@CS–TDI–Titriplex V nanomaterial (1)

In a 50 mL round-bottomed flask, toluene diisocyanate (TDI) (d = 1.214 g cm^{-3}, 1.2 mmol, 1.46 mL) was added dropwise to a suspension containing Titriplex V (1.0 mmol, 0.394 mg) and acetonitrile dried on 4A zeolite molecular sieves (10 mL). Then, the mixture was stirred continuously in a N_2 atmosphere at 80 °C for 24 h. After that, Fe_3O_4@CS (0.3 gr) was added to the mixture and stirred under reflux conditions for 24 h. Then, the obtained solid was filtered off and washed several times with acetonitrile. Finally, the obtained brown solid material was dried in a vacuum-drying oven at 40 °C for 5 h.

General procedure for the synthesis of acridinedione derivatives 5a–j catalyzed by the Fe_3O_4@CS–TDI–Titriplex V nanomaterial (1)

In a 5 mL round-bottomed flask, dimedone (2, 2.0 mmol), aldehyde (3a–j, 1.0 mmol), NH_4OAc (4, 1.2 mmol), and Fe_3O_4@CS–TDI–Titriplex V (1, 20.0 mg) were added to EtOH (96%, 2 mL). The obtained mixture was stirred under reflux conditions for the proper times indicated in Table 3. The progress of the reaction was monitored by TLC (eluent: EtOAc/n-hexane = 1/3). After completion of the reaction, EtOH (96%, 2.0 mL) was added to dissolve any solid product 5 under heating, and the solid catalyst 1 remained insoluble. The magnetic nanomaterial was separated by using an external magnet, and the filtrate was allowed to cool over time to obtain pure crystals of the desired products 5a–j. The separated catalyst 1 was suspended in acetone (1.0 mL), stirred for 30 minutes, and then filtered off. The obtained brown powder was heated in an oven at 60 °C for 1.5 h and reused for the next runs.

General procedure for the synthesis of 2-amino-3-cyano-4H-pyran derivatives 7a–j catalyzed by the Fe_3O_4@CS–TDI–Titriplex V nanomaterial (1)

In a 5 mL round-bottomed flask, dimedone (2, 1.0 mmol), aldehyde (3a–j, 1.0 mmol), malononitrile (6, 1.1 mmol), and Fe_3O_4@CS–TDI–Titriplex V (1, 20 mg) were added to EtOH (96%, 2 mL). The obtained mixture was stirred under reflux conditions for the times indicated in Table 4. The progress of the reaction was monitored by TLC (eluent: EtOAc : n-hexane, 1 : 2). After completion of the reaction, EtOH (96%, 2 mL) was added to dissolve any solid product 7 under heating, and the solid catalyst 1 remained insoluble. The magnetic nanocatalyst 1 was separated by using an external magnet, and the filtrate was allowed to cool over time to obtain pure crystals of the desired 2-amino-3-cyano-4H-pyrans (7). The separated catalyst was suspended in acetone (1 mL), stirred for 30 minutes, and then filtered off. The obtained brown powder was heated in an oven at 60 °C for 1.5 h and reused for the next runs.

Selected spectral data

9-(4-Chlorophenyl)-3,3,6,6-tetramethyl-3,4,6,7,9,10-hexahydroacridine-1,8(2H,5H)-dione (5a). Mp: 243–245 °C; IR (KBr, cm^{-1}): ν 3288, 3205, 3068, 2956, 2869, 1643, 1608, 1485, 1363, 1223, 1131. ^{1}H NMR (500 MHz, DMSO-d_6): δ (ppm) 0.85 (s, 6H), 0.99 (s, 6H), 1.96–1.99 (d, J = 12.8 Hz, 2H), 2.15–2.18 (d, J = 12.8 Hz, 2H), 2.30–2.33 (d, J = 14.9 Hz, 2H), 2.49–2.46 (d, J = 14.9 Hz, 2H), 4.77 (s, 1H, C–H$_{benzylic}$), 7.15–7.20 (m, 4H, H$_{aromatic}$), 9.33 (br s, 1H, N–H).

9-(4-Nitrophenyl)-3,3,6,6-tetramethyl-3,4,6,7,9,10-hexahydroacridine-1,8(2H,5H)-dione (5c). Mp: 302–304 °C, IR (KBr, cm^{-1}) ν 3384, 2958, 2908, 1643, 1602, 1514, 1447, 1364, 1221, 1171. ^{1}H NMR (500 MHz, DMSO-d_6): δ (ppm) 0.91 (s, 6H), 1.05 (s, 6H), 2.08–2.11 (d, J = 6.5 Hz, 2H), 2.27–2.30 (d, J = 6.5 Hz, 2H), 2.50–2.63 (m, 4H), 4.63 (s, 1H), 7.45–7.48 (m, 2H), 8.10–8.12 (m, 2H), 9.32 (s, 1H). Anal. calc. for $C_{23}H_{26}N_2O_4$; C 70.03, H 6.64, N 7.10, O 16.22; found: C 70.08, H 6.69, N 7.07, O 16.26.

2-Amino-7,7-dimethyl-4-(4-chlorophenyl)-5-oxo-5,6,7,8-tetrahydro-4H-pyran-3-carbonitrile (7a). Mp: 155–158 °C; IR (KBr, cm^{-1}): 3394, 3325, 2964, 2193, 1685, 1658, 1370, 1214. ^{1}H NMR (500 MHz, DMSO-d_6): δ (ppm) 0.92 (s, 3H), 1.01 (s, 3H), 2.08 (d, J = 16.1 Hz, 1H), 2.22 (d, J = 16.1 Hz, 1H), 2.47–2.53 (m, 2H), 4.17 (s, 1H), 7.03 (s, 2H), 7.15 (d, J = 8.4 Hz, 2H), 7.32 (d, J = 8.4 Hz, 1H).

Conclusions

In summary, we have developed a simple procedure for the preparation of a nanomagnetic solid acid hybrid material by using a chitosan biopolymer, a toluene-2,4-diisocyanate linker and diethylenetriaminepentaacetic acid (Fe_3O_4@CS–TDI–Titriplex V). The obtained nanomaterial was employed as an effective nano-ordered organocatalyst for the synthesis of 9-(aryl)-3,3,6,6-tetramethyl-3,4,6,7,9,10-hexahydroacridine-1,8(2H,5H)-dione and 2-amino-4-(4-aryl)-7,7-dimethyl-5-oxo-5,6,7,8-tetrahydro-4H-pyran-3-carbonitrile derivatives. The notable advantages of this method are clean reaction profiles, short reaction times, and high quantitative yields without the use of precious or toxic metals, which make it an improved and more practical alternative to the existing methods. Additionally, the catalyst could be simply separated and reused without any significant loss of its activity for at least four cycles.

Data availability

The data supporting this article have been included as part of the ESI.†

Conflicts of interest

There are no conflicts to declare.

Note added after first publication

This article replaces the version published on 2nd October 2024, which contained errors in Table 2 and Table 4. These

tables were incorrectly formatted during editing which led to the 'Aldehyde 3' and 'Product 5' entries in Table 2, and the 'Aldehyde 3' and 'Product 7' of Table 4, to be shown in an incorrect order and under the wrong column headings.

Acknowledgements

References

1 M. C. Roco, Nanotechnology: convergence with modern biology and medicine, *Curr. Opin. Biotechnol.*, 2003, **14**(3), 337–346, DOI: 10.1016/S0958-1669(03)00068-5.

2 A. Haleem, M. Javaid, R. P. Singh, S. Rab and R. Suman, Applications of nanotechnology in medical field: a brief review, *Global J. Health*, 2023, **7**(2), 70–77, DOI: 10.1016/j.glohj.2023.02.008.

3 S. Bayda, M. Adeel, T. Tuccinardi, M. Cordani and F. Rizzolio, The history of nanoscience and nanotechnology: from chemical–physical applications to nanomedicine, *Molecules*, 2019, **25**(1), 112.

4 T. F. Rambaran and A. Nordström, Medical and pharmacokinetic effects of nanopolyphenols: A systematic review of clinical trials, *Front. Food*, 2021, **2**(2), 140–152.

5 G. A. Mansoori and T. F. Soelaiman, *Nanotechnology-An Introduction for the Standards Community*, ASTM International, 2005.

6 K. Wang, F. Zhang, K. Xu, Y. Che, M. Qi and C. Song, Modified magnetic chitosan materials for heavy metal adsorption: a review, *RSC Adv.*, 2023, **13**(10), 6713–6736.

7 P. Evans, H. Matsunaga and M. Kiguchi, Large-scale application of nanotechnology for wood protection, *Nat. Nanotechnol.*, 2008, **3**(10), 577.

8 Y. Chen, A. Lavacchi, H. Miller, M. Bevilacqua, J. Filippi, M. Innocenti, A. Marchionni, W. Oberhauser, L. Wang and F. Vizza, Nanotechnology makes biomass electrolysis more energy efficient than water electrolysis, *Nat. Commun.*, 2014, **5**(1), 4036.

9 A. Bouafia, S. Meneceur, S. Chami, S. E. Laouini, H. Daoudi, S. Legmairi, H. A. Mohammed Mohammed, N. Aoun and F. Menaa, Removal of hydrocarbons and heavy metals from petroleum water by modern green nanotechnology methods, *Sci. Rep.*, 2023, **13**(1), 5637.

10 H. J. Squire, S. Tomatz, E. Voke, E. González-Grandío and M. Landry, The emerging role of nanotechnology in plant genetic engineering, *Nat. Rev. Bioeng.*, 2023, **1**(5), 314–328.

11 A. Almalik, H. Benabdelkamel, A. Masood, I. O. Alanazi, I. Alradwan, M. A. Majrashi, A. A. Alfadda, W. M. Alghamdi, H. Alrabiah and N. Tirelli, Hyaluronic acid coated chitosan nanoparticles reduced the immunogenicity of the formed protein corona, *Sci. Rep.*, 2017, **7**(1), 10542.

12 H. Jin, J. Pi, F. Yang, J. Jiang, X. Wang, H. Bai, M. Shao, L. Huang, H. Zhu and P. Yang, Folate-chitosan nanoparticles loaded with ursolic acid confer anti-breast cancer activities in vitro and in vivo, *Sci. Rep.*, 2016, **6**(1), 30782.

13 A. Zebardasti, M. G. Dekamin, E. Doustkhah and M. H. N. Assadi, Carbamate-Isocyanurate-Bridged Periodic Mesoporous Organosilica for van der Waals CO2 Capture, *Inorg. Chem.*, 2020, **59**(16), 11223–11227, DOI: 10.1021/acs.inorgchem.0c01449.

14 F. Mustafa and S. Andreescu, Nanotechnology-based approaches for food sensing and packaging applications, *RSC Adv.*, 2020, **10**(33), 19309–19336.

15 A. Yaghoubi and M. G. Dekamin, Green and Facile Synthesis of 4H-Pyran Scaffold Catalyzed by Pure Nano-Ordered Periodic Mesoporous Organosilica with Isocyanurate Framework (PMO-ICS), *ChemistrySelect*, 2017, **2**(28), 9236–9243.

16 M. G. Dekamin, F. Mehdipoor and A. Yaghoubi, 1,3,5-Tris (2-hydroxyethyl) isocyanurate functionalized graphene oxide: a novel and efficient nanocatalyst for the one-pot synthesis of 3,4-dihydropyrimidin-2 (1H)-ones, *New J. Chem.*, 2017, **41**(14), 6893–6901.

17 L. Gonzalez, R. J. Loza, K.-Y. Han, S. Sunoqrot, C. Cunningham, P. Purta, J. Drake, S. Jain, S. Hong and J.-H. Chang, Nanotechnology in corneal neovascularization therapy—a review, *J. Ocul. Pharmacol. Therapeut.*, 2013, **29**(2), 124–134.

18 R. C. Cioc, E. Ruijter and R. V. Orru, Multicomponent reactions: advanced tools for sustainable organic synthesis, *Green Chem.*, 2014, **16**(6), 2958–2975.

19 I. Eilks and F. Rauch, Sustainable development and green chemistry in chemistry education, *Chem. Educ. Res. Pract.*, 2012, **13**(2), 57–58, DOI: 10.1039/C2RP90003C.

20 K. N. Ganesh, D. Zhang, S. J. Miller, K. Rossen, P. J. Chirik, M. C. Kozlowski, J. B. Zimmerman, B. W. Brooks, P. E. Savage, D. T. Allen, *et al.*, Green Chemistry: A Framework for a Sustainable Future, *Environ. Sci. Technol. Lett.*, 2021, **8**(7), 487–491, DOI: 10.1021/acs.estlett.1c00434.

21 P. T. Anastas and J. B. Zimmerman, The United Nations sustainability goals: How can sustainable chemistry contribute?, *Curr. Opin. Green Sustainable Chem.*, 2018, **13**, 150–153.

22 A. Domling, W. Wang and K. Wang, Chemistry and biology of multicomponent reactions, *Chem. Rev.*, 2012, **112**(6), 3083–3135.

23 M. G. Dekamin, M. Azimoshan and L. Ramezani, Chitosan: a highly efficient renewable and recoverable bio-polymer catalyst for the expeditious synthesis of α-amino nitriles and imines under mild conditions, *Green Chem.*, 2013, **15**(3), 811–820.

24 M. G. Dekamin, M. Eslami and A. Maleki, Potassium phthalimide-N-oxyl: a novel, efficient, and simple organocatalyst for the one-pot three-component synthesis of various 2-amino-4H-chromene derivatives in water, *Tetrahedron*, 2013, **69**(3), 1074–1085.

25 M. G. Dekamin and Z. Mokhtari, Highly efficient and convenient Strecker reaction of carbonyl compounds and amines with TMSCN catalyzed by MCM-41 anchored sulfonic acid as a recoverable catalyst, *Tetrahedron*, 2012, **68**(3), 922–930.

26 M. G. Dekamin, S. Z. Peyman, Z. Karimi, S. Javanshir, M. R. Naimi-Jamal and M. Barikani, Sodium alginate: An efficient biopolymeric catalyst for green synthesis of 2-amino-4H-pyran derivatives, *Int. J. Biol. Macromol.*, 2016, **87**, 172–179.

27 N. Rostami, M. G. Dekamin, E. Valiey and H. Fanimoghadam, Chitosan-EDTA-Cellulose network as a green, recyclable and multifunctional biopolymeric organocatalyst for the one-pot synthesis of 2-amino-4 H-pyran derivatives, *Sci. Rep.*, 2022, **12**(1), 8642.

28 V. Raj and J. Lee, 2H/4H-Chromenes—A versatile biologically attractive Scaffold, *Front. Chem.*, 2020, **8**, 623.

29 H. Rouh, Y. Liu, N. Katakam, L. Pham, Y.-L. Zhu and G. Li, Synthesis of functionalized chromene and chroman derivatives via cesium carbonate promoted formal [4+2] annulation of 2′-hydroxychalcones with allenoates, *J. Org. Chem. USSR*, 2018, **83**(24), 15372–15379.

30 H. A. Khatab, S. F. Hammad, E. M. El-Fakharany, A. I. Hashem and E. A. El-Helw, Synthesis and cytotoxicity evaluation of novel 1,8-acridinedione derivatives bearing phthalimide moiety as potential antitumor agents, *Sci. Rep.*, 2023, **13**(1), 15093.

31 A. Alinasab Amiri, S. Javanshir, Z. Dolatkhah and M. G. Dekamin, SO3H-functionalized mesoporous silica materials as solid acid catalyst for facile and solvent-free synthesis of 2H-indazolo[2,1-b]phthalazine-1,6,11-trione derivatives, *New J. Chem.*, 2015, **39**(12), 9665–9671, DOI: 10.1039/C5NJ01733E.

32 A. Yaghoubi, M. G. Dekamin and B. Karimi, Propylsulfonic Acid-Anchored Isocyanurate-Based Periodic Mesoporous Organosilica (PMO-ICS-PrSO3H): A Highly Efficient and Recoverable Nanoporous Catalyst for the One-Pot Synthesis of Substituted Polyhydroquinolines, *Catal. Lett.*, 2017, **147**(10), 2656–2663, DOI: 10.1007/s10562-017-2159-5.

33 V. Polshettiwar, R. Luque, A. Fihri, H. Zhu, M. Bouhrara and J.-M. Basset, Magnetically recoverable nanocatalysts, *Chem. Rev.*, 2011, **111**(5), 3036–3075.

34 X. Cui, A.-E. Surkus, K. Junge, C. Topf, J. Radnik, C. Kreyenschulte and M. Beller, Highly selective hydrogenation of arenes using nanostructured ruthenium catalysts modified with a carbon–nitrogen matrix, *Nat. Commun.*, 2016, **7**(1), 11326.

35 L. Liu and A. Corma, Metal catalysts for heterogeneous catalysis: from single atoms to nanoclusters and nanoparticles, *Chem. Rev.*, 2018, **118**(10), 4981–5079.

36 N. Nikooei, M. G. Dekamin and E. Valiey, Benzene-1,3,5-tricarboxylic acid-functionalized MCM-41 as a novel and recoverable hybrid catalyst for expeditious and efficient synthesis of 2,3-dihydroquinazolin-4(1H)-ones via one-pot three-component reaction, *Res. Chem. Intermed.*, 2020, **46**(8), 3891–3909.

37 Z. Alirezvani, M. G. Dekamin and E. Valiey, Cu (II) and magnetite nanoparticles decorated melamine-functionalized chitosan: A synergistic multifunctional catalyst for sustainable cascade oxidation of benzyl alcohols/Knoevenagel condensation, *Sci. Rep.*, 2019, **9**(1), 17758.

38 X. Zheng, S. Luo, L. Zhang and J.-P. Cheng, Magnetic nanoparticle supported ionic liquid catalysts for CO2 cycloaddition reactions, *Green Chem.*, 2009, **11**(4), 455–458.

39 M. Ishani, M. G. Dekamin and Z. Alirezvani, Superparamagnetic silica core-shell hybrid attached to graphene oxide as a promising recoverable catalyst for expeditious synthesis of TMS-protected cyanohydrins, *J. Colloid Interface Sci.*, 2018, **521**, 232–241.

40 B. Fattahi and M. G. Dekamin, Fe$_3$O$_4$/SiO$_2$ decorated trimesic acid-melamine nanocomposite: a reusable supramolecular organocatalyst for efficient multicomponent synthesis of imidazole derivatives, *Sci. Rep.*, 2023, **13**(1), 401.

41 S. Laurent, D. Forge, M. Port, A. Roch, C. Robic, L. Vander Elst and R. N. Muller, Magnetic iron oxide nanoparticles: synthesis, stabilization, vectorization, physicochemical characterizations, and biological applications, *Chem. Rev.*, 2008, **108**(6), 2064–2110.

42 Y. Shen, J. Tang, Z. Nie, Y. Wang, Y. Ren and L. Zuo, Preparation and application of magnetic Fe3O4 nanoparticles for wastewater purification, *Separ. Purif. Technol.*, 2009, **68**(3), 312–319.

43 A. R. Liandi, A. H. Cahyana, R. T. Yunarti and T. P. Wendari, Facile synthesis of magnetic Fe3O4@Chitosan nanocomposite as environmentally green catalyst in multicomponent Knoevenagel-Michael domino reaction, *Ceram. Int.*, 2022, **48**(14), 20266–20274.

44 J. Baranwal, B. Barse, A. Fais, G. L. Delogu and A. Kumar, Biopolymer: A sustainable material for food and medical applications, *Polymers*, 2022, **14**(5), 983.

45 J. M. Ruso and P. V. Messina, *Biopolymers for Medical Applications*, CRC Press, 2017.

46 N. Raghav, M. R. Sharma and J. F. Kennedy, Nanocellulose: A mini-review on types and use in drug delivery systems, *Carbohydr. Polym. Technol. Appl.*, 2021, **2**, 100031.

47 V. Siracusa, P. Rocculi, S. Romani and M. Dalla Rosa, Biodegradable polymers for food packaging: a review, *Trends Food Sci. Technol.*, 2008, **19**(12), 634–643.

48 S. Biswas and A. Pal, Application of biopolymers as a new age sustainable material for surfactant adsorption: A brief review, *Carbohydr. Polym. Technol. Appl.*, 2021, **2**, 100145.

49 C. B. Godiya, S. Kumar and B. J. Park, Superior catalytic reduction of methylene blue and 4-nitrophenol by copper nanoparticles-templated chitosan nanocatalyst, *Carbohydr. Polym. Technol. Appl.*, 2023, **5**, 100267.

50 N. Peelman, P. Ragaert, B. De Meulenaer, D. Adons, R. Peeters, L. Cardon, F. Van Impe and F. Devlieghere, Application of bioplastics for food packaging, *Trends Food Sci. Technol.*, 2013, **32**(2), 128–141.

51 M. M. El-Sayed, R. E. Elsayed, A. Attia, H. H. Farghal, R. A. Azzam and T. M. Madkour, Novel nanoporous

membranes of bio-based cellulose acetate, poly (lactic acid) and biodegradable polyurethane in-situ impregnated with catalytic cobalt nanoparticles for the removal of Methylene Blue and Congo Red dyes from wastewater, *Carbohydr. Polym. Technol. Appl.*, 2021, **2**, 100123.

52 N. Rostami, M. G. Dekamin and E. Valiey, Chitosan-EDTA-Cellulose bio-based network: A recyclable multifunctional organocatalyst for green and expeditious synthesis of Hantzsch esters, *Carbohydr. Polym. Technol. Appl.*, 2023, **5**, 100279.

53 T. Chen, Y. Peng, M. Qiu, C. Yi and Z. Xu, Recent advances in mixing-induced nanoprecipitation: from creating complex nanostructures to emerging applications beyond biomedicine, *Nanoscale*, 2023, **15**(8), 3594–3609.

54 M. Dohendou, K. Pakzad, Z. Nezafat, M. Nasrollahzadeh and M. G. Dekamin, Progresses in chitin, chitosan, starch, cellulose, pectin, alginate, gelatin and gum based (nano) catalysts for the Heck coupling reactions: A review, *Int. J. Biol. Macromol.*, 2021, **192**, 771–819.

55 P. Shakib, M. G. Dekamin, E. Valiey, S. Karami and M. Dohendou, Ultrasound-Promoted preparation and application of novel bifunctional core/shell Fe3O4@SiO2@ PTS-APG as a robust catalyst in the expeditious synthesis of Hantzsch esters, *Sci. Rep.*, 2023, **13**(1), 8016.

56 M. Dohendou, M. G. Dekamin and D. Namaki, Supramolecular Pd@ methioine-EDTA-chitosan nanocomposite: an effective and recyclable bio-based and eco-friendly catalyst for the green Heck cross-coupling reaction under mild conditions, *Nanoscale Adv.*, 2023, **5**(13), 3463–3484.

57 E. Valiey, M. G. Dekamin and S. Bondarian, Sulfamic acid grafted to cross-linked chitosan by dendritic units: A bio-based, highly efficient and heterogeneous organocatalyst for green synthesis of 2,3-dihydroquinazoline derivatives, *RSC Adv.*, 2023, **13**(1), 320–334.

58 Y. Zeng, S. Zhao, S. Yang and S.-Y. Ding, Lignin plays a negative role in the biochemical process for producing lignocellulosic biofuels, *Curr. Opin. Biotechnol.*, 2014, **27**, 38–45.

59 D. M. Arias, E. Ortíz-Sánchez, P. U. Okoye, H. Rodríguez-Rangel, A. B. Ortega, A. Longoria, R. Domínguez-Espíndola and P. Sebastian, A review on cyanobacteria cultivation for carbohydrate-based biofuels: cultivation aspects, polysaccharides accumulation strategies, and biofuels production scenarios, *Sci. Total Environ.*, 2021, **794**, 148636.

60 J. Safari and L. Javadian, Chitosan decorated Fe3O4 nanoparticles as a magnetic catalyst in the synthesis of phenytoin derivatives, *RSC Adv.*, 2014, **4**(90), 48973–48979.

61 Z. Zarnegar and J. Safari, Fe3O4@ chitosan nanoparticles: a valuable heterogeneous nanocatalyst for the synthesis of 2,4,5-trisubstituted imidazoles, *RSC Adv.*, 2014, **4**(40), 20932–20939.

62 S. Ilkhanizadeh, J. Khalafy and M. G. Dekamin, Sodium alginate: Abiopolymeric catalyst for the synthesis of novel and known polysubstituted pyrano[3,2-c]chromenes, *Int. J. Biol. Macromol.*, 2019, **140**, 605–613.

63 B. Fattahi and M. G. Dekamin, Cu(II)/citric acid grafted to chitosan by dendritic units of melamine as a novel and highly efficient heterogeneous catalyst for the synthesis of 2-aminobenzothiazole derivatives, *Colloid Interface Sci. Commun.*, 2023, **54**, 100711.

64 Y. N. Malyar, N. Y. Vasilyeva, A. S. Kazachenko, V. S. Borovkova, A. M. Skripnikov, A. V. Miroshnikova, D. V. Zimonin, V. A. Ionin, A. S. Kazachenko and N. Issaoui, Modification of arabinogalactan isolated from Larix sibirica Ledeb. into sulfated derivatives with the controlled molecular weights, *Molecules*, 2021, **26**(17), 5364.

65 B. Banerjee, Recent developments on ultrasound-assisted one-pot multicomponent synthesis of biologically relevant heterocycles, *Ultrason. Sonochem.*, 2017, **35**, 15–35.

66 N. Kaur, Ultrasound-assisted green synthesis of five-membered O-and S-heterocycles, *Synth. Commun.*, 2018, **48**(14), 1715–1738.

67 L. Mallu, D. Thirumalai and I. V. Asharani, One-pot cascade synthesis and in vitro evaluation of anti-inflammatory and antidiabetic activities of S-methylphenyl substituted acridine-1,8-diones, *Chem. Biol. Drug Des.*, 2017, **90**(4), 520–526.

68 R. Sarkar and C. Mukhopadhyay, Cross-dehydrogenative regioselective Csp3–Csp2 coupling of enamino-ketones followed by rearrangement: an amazing formation route to acridine-1,8-dione derivatives, *Org. Biomol. Chem.*, 2016, **14**(9), 2706–2715, DOI: **10.1039/C5OB02655E**.

69 Y. M. Shchekotikhin, T. Nikolaeva, G. Shub and A. Kriven'ko, Synthesis and antimicrobial activity of substituted 1, 8-dioxodecahydroacridines, *Pharmaceut. Chem. J.*, 2001, **35**(4), 206–208.

70 A. Pyrko, Synthesis and transformations of new 1,2,3,4,5,6,7,8,9,10-decahydroacridine-1,8-dione derivatives, *Russ. J. Org. Chem.*, 2008, **44**, 1215–1224.

71 N. Iqbal, S. A. Ali, I. Munir, S. Khan, K. Ayub, M. al-Rashida, M. Islam, Z. Shafiq, R. Ludwig and A. Hameed, Acridinedione as selective flouride ion chemosensor: a detailed spectroscopic and quantum mechanical investigation, *RSC Adv.*, 2018, **8**(4), 1993–2003, DOI: **10.1039/C7RA11974G**.

72 M. Odabaşoğlu, M. Kaya, O. Büyükgüngör, Y. Yıldırır and L. Türker, 9-(4-Methoxyphenyl)-3,3,6,6-tetramethyl-10-p-tolyl-1,2,3,4,5,6,7,8,9,10-decahydroacridine-1, 8-dione, *Acta Crystallogr., Sect. E: Struct. Rep. Online*, 2007, **63**(4), o1763–o1765.

73 L. B. Li, S. J. Ji and Y. Liu, A New Fluorescent Chemosensor for Cu2+ Based on 1,2,3,4,5,6,7,8,9,10-Decahydroacridine-1,8-dione Fluorophore, *Chin. J. Chem.*, 2008, **26**(6), 979–982.

74 A. H. Halawa, M. M. Elaasser, A. M. El Kerdawy, A. M. Abd El-Hady, H. A. Emam and A. M. El-Agrody, Anticancer activities, molecular docking and structure–activity relationship of novel synthesized 4H-chromene, and 5H-chromeno [2,3-d] pyrimidine candidates, *Med. Chem. Res.*, 2017, **26**, 2624–2638.

75 V. Luque-Agudo, J. Albarrán-Velo, M. E. Light, J. M. Padrón, E. Román, J. A. Serrano and M. V. Gil, Synthesis and antiproliferative activity of new 2-glyco-3-nitro-2H-chromenes, *Bioorg. Chem.*, 2019, **87**, 112–116.

76 T. H. Afifi, R. M. Okasha, H. E. Ahmed, J. Ilaš, T. Saleh and A. S. Abd-El-Aziz, Structure-activity relationships and molecular docking studies of chromene and chromene based azo chromophores: A novel series of potent antimicrobial and anticancer agents, *EXCLI J.*, 2017, **16**, 868.

77 M. Mashhadinezhad, M. Mamaghani, M. Rassa and F. Shirini, A facile green synthesis of chromene derivatives as antioxidant and antibacterial agents through a modified natural soil, *ChemistrySelect*, 2019, **4**(17), 4920–4932.

78 M. B. Tehrani, Z. Rezaei, M. Asadi, H. Behnammanesh, H. Nadri, F. Afsharirad, A. Moradi, B. Larijani, M. Mohammadi-Khanaposhtani and M. Mahdavi, Design, synthesis, and cholinesterase inhibition assay of coumarin-3-carboxamide-N-morpholine hybrids as new anti-Alzheimer agents, *Chem. Biodiversity*, 2019, **16**(7), e1900144.

79 A. Chaudhary, K. Singh, N. Verma, S. Kumar, D. Kumar and P. P. Sharma, Chromenes-a novel class of heterocyclic compounds: Recent advancements and future directions, *Mini Rev. Med. Chem.*, 2022, **22**(21), 2736–2751.

80 Y. He, R. Hu, R. Tong, F. Li, J. Shi and M. Zhang, K2CO3-Mediated Synthesis of Functionalised 4-Substituted-2-amino-3-cyano-4H-chromenes via Michael-Cyclization Reactions, *Molecules*, 2014, **19**(12), 19253–19268.

81 G.-W. Wang and C.-B. Miao, Environmentally benign one-pot multi-component approaches to the synthesis of novel unsymmetrical 4-arylacridinediones, *Green Chem.*, 2006, **8**(12), 1080–1085.

82 A. Poursattar Marjani, B. Ebrahimi Saatluo and F. Nouri, An efficient synthesis of 4H-chromene derivatives by a one-pot, three-component reaction, *Iran. J. Chem. Chem. Eng.*, 2018, **37**(1), 149–157.

83 N. Madankumar and K. Pitchumani, β-Cyclodextrin monosulphonic acid promoted multicomponent synthesis of 1,8-dioxodecahydroacridines in water, *ChemistrySelect*, 2018, **3**(39), 10886–10891.

84 T. A. J. Siddiqui, S. F. Shaikh, B. B. Totawar, M. Dumpala, M. Ubaidullah, B. M. Thamer, R. S. Mane and A. M. Al-Enizi, Tungsten oxides: green and sustainable heterogeneous nanocatalysts for the synthesis of bioactive heterocyclic compounds, *Dalton Trans.*, 2021, **50**(6), 2032–2041, DOI: **10.1039/D0DT04238B**.

85 B. Aday, Y. Yıldız, R. Ulus, S. Eris, F. Sen and M. Kaya, One-pot, efficient and green synthesis of acridinedione derivatives using highly monodisperse platinum nanoparticles supported with reduced graphene oxide, *New J. Chem.*, 2016, **40**(1), 748–754, DOI: **10.1039/C5NJ02098K**.

86 S. T. Atkore, P. V. Raithak, K. Vijay, S. A. Ansari, I. A. Ansari and R. Varala, Highly Efficient Bimetallic Catalyst for the Synthesis of N-substituted Decahydroacridine-1, 8-diones

and Xanthene-1, 8-diones: Evaluation of their Biological Activity, *Curr. Org. Synth.*, 2024, **21**(3), 345–356.

87 B. Sardar, R. Jamatia, D. Pal and D. Srimani, Multicomponent Dehydrogenative Synthesis of Acridine-1,8-diones Catalyzed by Ru-doped Hydrotalcite, *Asian J. Org. Chem.*, 2021, **10**(8), 2195–2204, DOI: **10.1002/ajoc.202100286**.

88 Z. Sabri, N. Shadjou and M. Mahmoudian, Accelerated synthesis of 1,8-dioxo-octahydroxanthene and 1,8-dioxo-decahydroacridine derivatives using dendritic mesoporous nanosilica functionalized by hexamethylenetetramine: a novel nanocatalyst, *RSC Adv.*, 2024, **14**(4), 2633–2651, DOI: **10.1039/D3RA07629F**.

89 K. B. Ramesh and M. A. Pasha, Study on one-pot four-component synthesis of 9-aryl-hexahydro-acridine-1,8-diones using SiO2–I as a new heterogeneous catalyst and their anticancer activity, *Bioorg. Med. Chem. Lett.*, 2014, **24**(16), 3907–3913, DOI: **10.1016/j.bmcl.2014.06.047**.

90 A. Zhu, R. Liu, C. Du and L. Li, Betainium-based ionic liquids catalyzed multicomponent Hantzsch reactions for the efficient synthesis of acridinediones, *RSC Adv.*, 2017, **7**(11), 6679–6684, DOI: **10.1039/C6RA25709G**.

91 A. Bamoniri and S. Fouladgar, SnCl4-functionalized nano-Fe3O4 encapsulated-silica particles as a novel heterogeneous solid acid for the synthesis of 1,4-dihydropyridine derivatives, *RSC Adv.*, 2015, **5**(96), 78483–78490.

92 Z. Zarei and B. Akhlaghinia, ZnII doped and immobilized on functionalized magnetic hydrotalcite (Fe3O4/HT-SMTU-ZnII): a novel, green and magnetically recyclable bifunctional nanocatalyst for the one-pot multi-component synthesis of acridinediones under solvent-free conditions, *New J. Chem.*, 2017, **41**(24), 15485–15500, DOI: **10.1039/C7NJ03281A**.

93 M. Sam, M. G. Dekamin and Z. Alirezvani, Dendrons containing boric acid and 1, 3, 5-tris (2-hydroxyethyl) isocyanurate covalently attached to silica-coated magnetite for the expeditious synthesis of Hantzsch esters, *Sci. Rep.*, 2021, **11**(1), 2399.

94 P. Mahajabeen and A. Chadha, A novel green route for the synthesis of N-phenylacetamides, benzimidazoles and acridinediones using Candida parapsilosis ATCC 7330, *RSC Adv.*, 2013, **3**(44), 21972–21980, DOI: **10.1039/C3RA44058C**.

95 M. R. Maurya, N. Kumar and F. Avecilla, Controlled Modification of Triaminoguanidine-Based μ3 Ligands in Multinuclear [VIVO]/[VVO2] Complexes and Their Catalytic Potential in the Synthesis of 2-Amino-3-cyano-4H-pyrans/4H-chromenes, *Inorg. Chem.*, 2024, **63**(5), 2505–2524, DOI: **10.1021/acs.inorgchem.3c03704**.

96 F. Kalantari, A. Ramazani, M. R. Poor Heravi, H. Aghahosseini and K. Ślepokura, Magnetic Nanoparticles Functionalized with Copper Hydroxyproline Complexes as an Efficient, Recoverable, and Recyclable Nanocatalyst: Synthesis and Its Catalytic Application in a Tandem Knoevenagel–Michael Cyclocondensation

Reaction, *Inorg. Chem.*, 2021, **60**(19), 15010–15023, DOI: 10.1021/acs.inorgchem.1c02470.

97 F. Ghobakhloo, D. Azarifar, M. Mohammadi, H. Keypour and H. Zeynali, Copper(II) Schiff-Base Complex Modified UiO-66-NH2(Zr) Metal–Organic Framework Catalysts for Knoevenagel Condensation–Michael Addition–Cyclization Reactions, *Inorg. Chem.*, 2022, **61**(12), 4825–4841, DOI: 10.1021/acs.inorgchem.1c03284.

98 N. Farzaneh, F. Radinekiyan, M. R. Naimi-Jamal and M. G. Dekamin, Development of new magnetic nanocomposite designed by reduced graphene oxide aerogel and HKUST-1, and its catalytic application in the synthesis of polyhydroquinoline and 1,8-dioxo-decahydroacridine derivatives, *Sci. Rep.*, 2023, **13**(1), 22913, DOI: 10.1038/s41598-023-48674-5.

99 Y. Merroun, S. Chehab, A. E. Hallaoui, T. Guedira, S. Boukhris, A. Souizi and R. Ghailane, A new heterogeneous catalyst of triple superphosphate/titanium tetrachloride is used for the synthesis of 1,8-dioxooctahydroxanthenes and tetrahydrobenzo[b]pyrans, *J. Mol. Struct.*, 2023, **1294**, 136554, DOI: 10.1016/j.molstruc.2023.136554.

100 S. Saneinezhad, L. Mohammadi, V. Zadsirjan, F. F. Bamoharram and M. M. Heravi, Silver nanoparticles-decorated Preyssler functionalized cellulose biocomposite as a novel and efficient catalyst for the synthesis of 2-amino-4H-pyrans and spirochromenes, *Sci. Rep.*, 2020, **10**(1), 14540, DOI: 10.1038/s41598-020-70738-z.

101 N. Rahman, N. Kushwah and K. I. Priyadarsini, A redox active organodiselenide as an efficacious catalyst for the synthesis of oxygen-containing heterocyclic compounds, *New J. Chem.*, 2023, **47**(33), 15686–15693, DOI: 10.1039/D3NJ01423A.

102 Y. R. Shelke, V. D. Bobade, D. R. Tope, J. A. Agashe and A. V. A. Borhade, Simple, Green, and Efficient One-Pot Synthesis of Dihydro-pyrano[3,2-c]chromene Derivatives Using MgMnO3@ZrO2@CoO as a Core–Shell Nanocrystalline Catalyst, *Russ. J. Org. Chem.*, 2023, **59**(4), 663–673, DOI: 10.1134/S1070428023040152.

103 M. R. P. Heravi, P. Aghamohammadi and E. Vessally, Green synthesis and antibacterial, antifungal activities of 4H-pyran, tetrahydro-4H-chromenes and spiro2-oxindole derivatives by highly efficient Fe3O4@ SiO2@ NH2@ Pd (OCOCH3)2 nanocatalyst, *J. Mol. Struct.*, 2022, **1249**, 131534.

104 F. Matloubi Moghaddam, M. Eslami and G. Hoda, Cysteic acid grafted to magnetic graphene oxide as a promising recoverable solid acid catalyst for the synthesis of diverse 4H-chromene, *Sci. Rep.*, 2020, **10**(1), 20968, DOI: 10.1038/s41598-020-77872-8.

105 A. Maleki, H. Movahed, P. Ravaghi and T. Kari, Facile in situ synthesis and characterization of a novel PANI/Fe3O4/Ag nanocomposite and investigation of catalytic applications, *RSC Adv.*, 2016, **6**(101), 98777–98787, DOI: 10.1039/C6RA18185F.

106 F. Shirini and N. Daneshvar, Introduction of taurine (2-aminoethanesulfonic acid) as a green bio-organic catalyst for the promotion of organic reactions under green conditions, *RSC Adv.*, 2016, **6**(111), 110190–110205, DOI: 10.1039/C6RA15432H.

107 S. Saini, M. Mayank, N. Kaur and N. Singh, A cytochrome c-urea functionalized dipeptide conjugate: an efficient HBD framework to synthesize 4H-pyrans via one-pot multicomponent reaction, *Green Chem.*, 2020, **22**(3), 956–968, DOI: 10.1039/C9GC03512E.

108 M. G. Dekamin and M. Eslami, Highly efficient organocatalytic synthesis of diverse and densely functionalized 2-amino-3-cyano-4H-pyrans under mechanochemical ball milling, *Green Chem.*, 2014, **16**(12), 4914–4921, DOI: 10.1039/C4GC00411F.

109 H. Wu, Z. Wang and L. Tao, The Hantzsch reaction in polymer chemistry: synthesis and tentative application, *Polym. Chem.*, 2017, **8**(47), 7290–7296.

110 Q. Zhang, Y. Zhao, B. Yang, C. Fu, L. Zhao, X. Wang, Y. Wei and L. Tao, Lighting up the PEGylation agents via the Hantzsch reaction, *Polym. Chem.*, 2016, **7**(3), 523–528.

111 A. Malihishoja, M. G. Dekamin and M. Eslami, Magnetic polyborate nanoparticles as a green and efficient catalyst for one-pot four-component synthesis of highly substituted imidazole derivatives, *RSC Adv.*, 2023, **13**(24), 16584–16601.

112 M. Dohendou, M. G. Dekamin and D. Namaki, Pd@ l-asparagine–EDTA–chitosan: a highly effective and reusable bio-based and biodegradable catalyst for the Heck cross-coupling reaction under mild conditions, *Nanoscale Adv.*, 2023, **5**(9), 2621–2638.

113 R. P. Sourkouhi, M. G. Dekamin, E. Valiey and M. Dohendou, Magnetic decorated 5-sulfosalicylic acid grafted to chitosan: A solid acid organocatalyst for green synthesis of quinazoline derivatives, *Carbohydr. Polym. Technol. Appl.*, 2024, **7**, 100420, DOI: 10.1016/j.carpta.2023.100420.

114 M. G. Dekamin, J. Mokhtari and M. R. Naimi-Jamal, Organocatalytic cyanosilylation of carbonyl compounds by tetrabutylammonium phthalimide-N-oxyl, *Catal. Commun.*, 2009, **10**(5), 582–585, DOI: 10.1016/j.catcom.2008.10.036.

115 I. S. Blagbrough, N. E. Mackenzie, C. Ortiz and A. I. Scott, The condensation reaction between isocyanates and carboxylic acids. A practical synthesis of substituted amides and anilides, *Tetrahedron Lett.*, 1986, **27**(11), 1251–1254, DOI: 10.1016/S0040-4039(00)84230-6.

116 C. Gürtler and K. Danielmeier, A catalyst system for the reaction of carboxylic acids with aliphatic isocyanates, *Tetrahedron Lett.*, 2004, **45**(12), 2515–2521, DOI: 10.1016/j.tetlet.2004.02.012.

117 M. G. Dekamin, K. Varmira, M. Farahmand, S. Sagheb-Asl and Z. Karimi, Organocatalytic, rapid and facile cyclotrimerization of isocyanates using tetrabutylammonium phthalimide-N-oxyl and tetraethylammonium 2-(carbamoyl)benzoate under solvent-free conditions, *Catal. Commun.*, 2010, **12**(3), 226–230, DOI: 10.1016/j.catcom.2010.08.018.

118 E. Kovács, B. Rózsa, A. Csomos, I. G. Csizmadia and Z. Mucsi, Amide Activation in Ground and Excited States, *Molecules*, 2018, **23**(11), 2859.

119 R. Beiranvand and M. G. Dekamin, Trimesic acid-functionalized chitosan: A novel and efficient multifunctional organocatalyst for green synthesis of polyhydroquinolines and acridinediones under mild conditions, *Heliyon*, 2023, **9**(6), e16315.

120 H. Alinezhad, M. Tajbakhsh, M. Norouzi, S. Baghery and J. Rakhtshah, Green and expeditious synthesis of 1,8-dioxodecahydroacridine derivatives catalysed by protic pyridinium ionic liquid, *J. Chem. Sci.*, 2013, **125**, 1517–1522.

121 D. Patil, D. Chandam, A. Mulik, P. Patil, S. Jagadale, R. Kant, V. Gupta and M. Deshmukh, Novel Brønsted acidic ionic liquid ([CMIM][CF 3 COO]) prompted multicomponent hantzsch reaction for the eco-friendly synthesis of acridinediones: An efficient and recyclable catalyst, *Catal. Lett.*, 2014, **144**, 949–958.

122 S.-J. Yü, S. Wu, X.-M. Zhao and C.-W. Lü, Green and efficient synthesis of acridine-1,8-diones and hexahydroquinolines via a KH2PO4 catalyzed Hantzsch-type reaction in aqueous ethanol, *Res. Chem. Intermed.*, 2017, **43**, 3121–3130.

123 X. Fan, Y. Li, X. Zhang, G. Qu and J. Wang, An efficient and green preparation of 9-arylacridine-1, 8-dione derivatives, *Heteroat. Chem.*, 2007, **18**(7), 786–790.

124 G.-W. Wang, J.-J. Xia, C.-B. Miao and X.-L. Wu, Environmentally friendly and efficient synthesis of various 1, 4-dihydropyridines in pure water, *Bull. Chem. Soc. Jpn.*, 2006, **79**(3), 454–459.

125 G. M. Ziarani, A. Badiei, M. Hassanzadeh and S. Mousavi, Synthesis of 1,8-dioxo-decahydroacridine derivatives using sulfonic acid functionalized silica (SiO2-Pr-SO3H) under solvent free conditions, *Arab. J. Chem.*, 2014, **7**(3), 335–339.

126 H.-P. Steinrueck and P. Wasserscheid, Ionic liquids in catalysis, *Catal. Lett.*, 2015, **145**, 380–397.

127 P. Sharma, M. Gupta, R. Kant and V. K. Gupta, One-pot synthesis of various 2-amino-4 H-chromene derivatives using a highly active supported ionic liquid catalyst, *RSC Adv.*, 2016, **6**(38), 32052–32059.

128 M. Abaszadeh and M. Seifi, Sodium benzenesulfinates: Novel and effective organo catalyst for three component synthesis 5, 6, 7, 8-Tetrahydro-4H-chromene derivatives under ultrasound irradiation, *Lett. Org. Chem.*, 2015, **12**(4), 271–276.

129 C. S. Maheswari, R. Ramesh and A. Lalitha, Synthesis, characterization, and catalytic behavior of bamboo rice husk ash, *J. Chin. Chem. Soc.*, 2017, **64**(8), 889–895.

130 A. Maleki, H. Movahed, P. Ravaghi and T. Kari, Facile in situ synthesis and characterization of a novel PANI/Fe 3 O 4/Ag nanocomposite and investigation of catalytic applications, *RSC Adv.*, 2016, **6**(101), 98777–98787.

131 S. M. Nezhad, S. A. Pourmousavi and E. N. Zare, Synthesis of Polyhydroquinolines and 2-Amino-4H-Chromenes and their Alkylene Bridging Derivatives using Sulfonic acid Functionalized Heterogeneous Nanocatalyst Based on Modified Poly (Styrene-alt-Maleic Anhydride), *Lett. Org. Chem.*, 2022, **19**(7), 542–557.

132 E. Abbaspour-Gilandeh, M. Aghaei-Hashjin, A. Yahyazadeh and H. Salemi, (CTA)3 [SiW12]–Li+–MMT: a novel, efficient and simple nanocatalyst for facile and one-pot access to diverse and densely functionalized 2-amino-4H-chromene derivatives via an eco-friendly multicomponent reaction in water, *RSC Adv.*, 2016, **6**(60), 55444–55462.

133 R. Gholami, A. Bamoniri and B. B. F. Mirjalili, One-pot synthesis of chromenes in the presence of nano-cellulose/Ti(IV)/Fe3O4 as natural-based magnetic nano-catalysts under solvent free conditions, *RSC Adv.*, 2022, **12**(42), 27555–27563.

134 F. Sameri, M. A. Bodaghifard and A. Mobinikhaledi, Zn (II)-Schiff base covalently anchored to CaO@SiO2: A hybrid nanocatalyst for green synthesis of 4H-pyrans, *Appl. Organomet. Chem.*, 2021, **35**(11), e6394.

135 I. Sehout, R. Boulcina, B. Boumoud, T. Boumoud and A. Debache, Solvent-free synthesis of polyhydroquinoline and 1, 8-dioxodecahydroacridine derivatives through the Hantzsch reaction catalyzed by a natural organic acid: A green method, *Synth. Commun.*, 2017, **47**(12), 1185–1191.

136 A. Amoozadeh, S. Golian and S. Rahmani, TiO2-coated magnetite nanoparticle-supported sulfonic acid as a new, efficient, magnetically separable and reusable heterogeneous solid acid catalyst for multicomponent reactions, *RSC Adv.*, 2015, **5**(57), 45974–45982.

137 A. T. Khan, M. Lal, S. Ali and M. M. Khan, One-pot three-component reaction for the synthesis of pyran annulated heterocyclic compounds using DMAP as a catalyst, *Tetrahedron Lett.*, 2011, **52**(41), 5327–5332, DOI: **10.1016/j.tetlet.2011.08.019**.

138 D. Shi, J. Mou, Q. Zhuang and X. Wang, One-pot synthesis of 2-amino-4-aryl-5-oxo-5,6,7,8-tetrahydro-4H-1-benzopyran-3-carbonitriles in aqueous media, *J. Chem. Res.*, 2004, **2004**(12), 821–823, DOI: **10.3184/0308234043431294**.